

Aluminum methyl and chloro complexes bearing monoanionic aminephenolate ligands: synthesis, characterization and use in polymerizations

Nduka Ikpo,^a Stephanie M. Barbon,^a Marcus W. Drover,^a Louise N. Dawe,^{a,b} and Francesca M. Kerton^{*a}

a. Department of Chemistry, Memorial University of Newfoundland, St. John's, NL, A1B 3X7, Canada

b. X-ray Crystallography Laboratory, Center for Chemical Analysis, Research and Training, Memorial University of Newfoundland, St. John's, NL, A1B 3X7, Canada

This is a postprint version of the article. Please cite as follows:

Nduka Ikpo, Stephanie M. Barbon, Marcus W. Drover, Louise N. Dawe, and Francesca M. Kerton. Aluminum Methyl and Chloro Complexes Bearing Monoanionic Aminephenolate Ligands: Synthesis, Characterization, and Use in Polymerizations, *Organometallics* 2012 31 (23), 8145-8158. <http://dx.doi.org/10.1021/om300757u>

Abstract:

A series of aluminum methyl and chloride complexes bearing 2(*N*-piperazinyl-*N'*-methyl)-2-methylene-4-*R'*-6-*R*-phenolate or 2(*N*-morpholinyl)-2-methylene-4-*R'*-6-*R*-phenolate

([ONE^{R¹,R²}]-) {[R¹ = *t*Bu, R² = Me, E = NMe (**L1**); R¹ = R² = *t*Bu, E = NMe (**L2**); R¹ = R² = *t*Bu,

E = O (**L3**)} ligands were synthesized and characterized through elemental analysis, ^1H , $^{13}\text{C}\{^1\text{H}\}$ and ^{27}Al NMR spectroscopy, and X-ray crystallography. Reactions of AlMe_3 with two equivalents of **L1H-L3H** gave $\{[\text{ONE}^{\text{R1,R2}}]_2\text{AlMe}\}$ (**1-3**) while reaction of Et_2AlCl with two equivalents **L1H** and **L3H** afforded $\{[\text{ONE}^{\text{R1,R2}}]_2\text{AlCl}\}$ (**4** and **5**) as monometallic complexes. The catalytic activity of complexes **1-3** toward ring-opening polymerization (ROP) of ϵ -caprolactone was assessed. These complexes are more active than analogous Zn complexes for this reaction but less active than the Zn analogs for ROP of *rac*-lactide. Characteristics of the polymer as well as polymerization kinetics and mechanism were studied. Polymer end-group analyses were achieved using ^1H NMR spectroscopy and MALDI-TOF MS. Eyring analyses were performed and the activation energies for the reactions were determined, which were significantly lower for **1** and **2** compared with **3**. This could be for several reasons: (1) the methylamine (NMe) group of **1** and **2**, which is a stronger base than the ether (O) group of **3**, might activate the incoming monomer via non-covalent interactions, and/or (2) the ether group is able to temporarily coordinate to the metal center and blocks the vacant coordination site towards incoming monomer, whilst the amine cannot do this. Preliminary studies using **4** and **5** towards copolymerization of cyclohexene oxide with carbon dioxide have been performed. **4** was inactive and **5** afforded polyethercarbonate (66.7% epoxide conversion, polymer contains 54.0% carbonate linkages).

Introduction

Biodegradable and biocompatible polyesters, such as poly(ϵ -caprolactone) (PCL), have attracted much attention due to their wide range of applications including environmentally friendly bulk packaging materials, implantable materials, sutures and as delivery media for controlled release

of drugs.¹⁻⁴ Ring-opening polymerization (ROP) of cyclic esters is mainly mediated by metal complexes which afford faster polymerization rates and greater control over molecular weight of the resulting polymers.⁵⁻⁸ Biocompatible metal complexes are important in the production of these polymers, where small amounts of catalyst may inevitably be incorporated.

Efforts by many research groups have focused on the development of biocompatible single-site metal initiators for ROP of ϵ -caprolactone and lactide with ligand design playing a profound role in this area. Well-designed ligands provide the ability to tune electronic and steric properties of the metal centers, which changes their reactivity. Thus, amine-phenolate and related ligands possessing a mixed set of N- and O- donor atoms have emerged as attractive candidates due to their ability to stabilize a wide range of metal centers and the ease of systematic steric manipulation by variation of the backbone and phenol substituents.⁹ A number of main-group and transition metal complexes including lithium,¹⁰⁻¹⁶ magnesium,¹⁷⁻²³ larger alkaline earths,²⁴ rare-earths,^{25,26} zinc,²⁷⁻³⁶ aluminum,³⁷⁻⁴⁴ tin,⁴⁵ zirconium^{46,47} and titanium⁴⁸ complexes stabilized by these and related ligands have been prepared and some are effective initiators for ROP of cyclic esters such as lactide and ϵ -caprolactone (e.g., **I-IV**, Figure 1). Among the catalysts/initiators studied, aluminum complexes with N,O- chelate and related ligands have attracted much attention due to their high activity and good polymer molecular weight control.^{4,49} For example, Dagorne and co-workers reported four-coordinate aluminum alkyl cationic complexes stabilized by a piperaziny aminephenolate ligand (e.g. Figure 1 **V**) which was employed in a preliminary study of propylene oxide ROP.³⁹ Five-coordinate aluminum complexes supported by mono anionic bidentate ketimate ligands have been investigated as catalysts for ROP of ϵ -caprolactone.⁵⁰ However, neutral five-coordinate piperaziny

aminephenolate aluminum species have not been reported in the literature for the polymerization of cyclic esters.

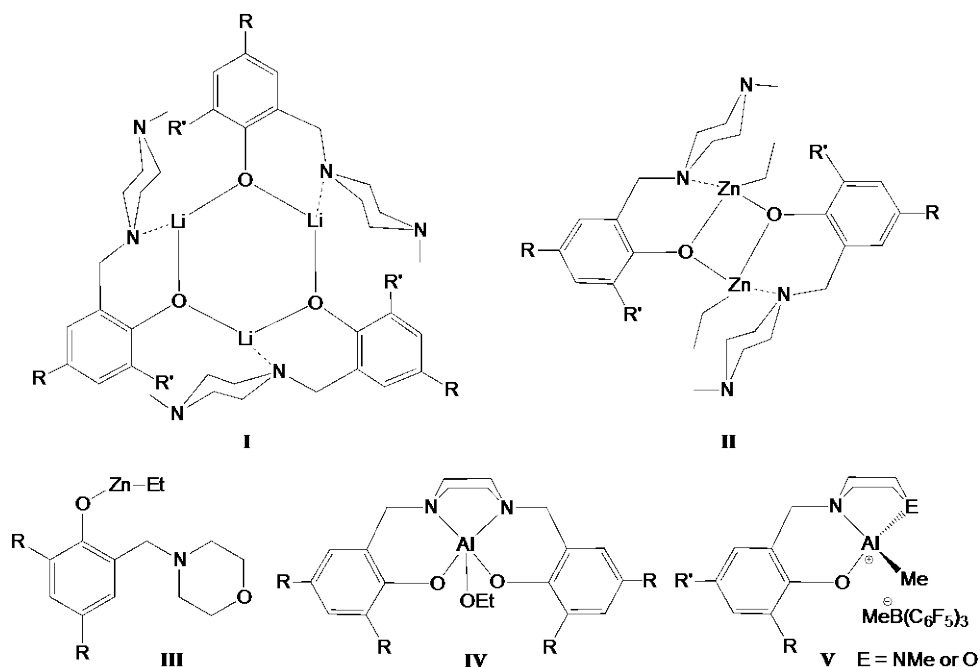


Figure 1. Some examples of previously reported piperazinyl and morpholinyl aminephenolate based complexes (R = alkyl or aryl).^{10,27,28,39,40}

Recently, we reported the synthesis of piperazinyl-aminephenolate zinc complexes (**II**), which showed good activity in ROP of rac-lactide and ϵ -caprolactone.²⁷ These zinc complexes, however, showed poor activity in the cycloaddition of carbon dioxide and epoxides. Lithium complexes (**I**) of the same ligand showed good activity in catalytic ROP of ϵ -caprolactone.¹⁰ Similarly, Carpentier, Sarazin and co-workers employed zinc complexes of a morpholinyl derived ligand (**III**) to achieve immortal ROP of cyclic esters.²⁸ The same group has investigated the reactivity of tin complexes of these ligands in immortal ROP of lactide and trimethylene carbonate.⁴⁵ In a recent study by Ma and Wang, aluminum complexes of quinoline-based ligands showed greater catalytic activity than corresponding Zn complexes in ROP of lactones,⁵¹ and

therefore we wanted to determine whether this was a general trend for bidentate ligand complexes of Al and Zn in ROP reactions. This contrasts with research using other ligands combined with Al and Zn where the Zn complexes usually show greater reactivity towards ROP of lactones.⁴ Using the activity scale developed by Redshaw and Arbaoui, which ranks metal complexes in these reactions from low to exceptional activities, most Al and Zn complexes exhibit low to good activity in ROP reactions.⁴ As Al and Zn systems are important due to their low toxicity, it is vital to gain further insights into their relative reactivity in order to design improved catalyst systems.

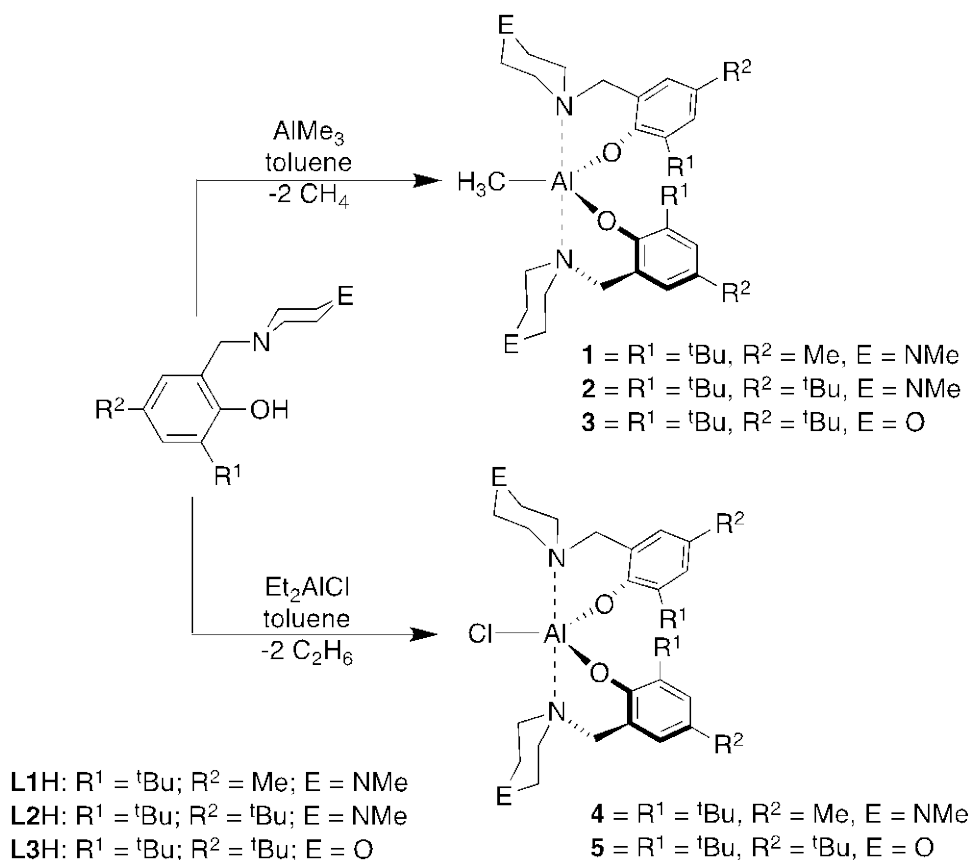
We are also interested in studying the effect of outersphere ligand substituents on polymerization reactions. Herein, we report the synthesis and characterization of five-coordinate aluminum alkyl/halide complexes bearing piperazinyl-aminephenolate ligands and their catalysis in the ROP of ϵ -caprolactone and preliminary results in carbon dioxide-cyclohexene oxide copolymerizations.

Results and Discussion

Synthesis and solid-state structures

The protio ligands were synthesized from the appropriate phenol, formaldehyde and 1-methylpiperazine or morpholine via a modified Mannich condensation reaction in water as described previously.^{27,52,53} The piperazinyl and morpholinyl aminephenol ligands differ in the nature of the E substituent, which is a methylamine (NMe) or ether (O) group respectively. Some complexes of these ligands (**L1-L3**) have been reported by our group and others, and will allow us to compare reactivity where data are available from these prior studies.^{10,27,28,31,32,39} Compounds **1-5** were synthesized through alkane elimination reactions using two equivalents of

the appropriate protio ligands with the corresponding alkyl/halide aluminum precursors (AlMe_3 or Et_2AlCl) in dry toluene as summarized in Scheme 1. Reactions of protio ligands $[\text{ONE}^{\text{R}^1\text{R}^2}]\text{H}$ with AlMe_3 in toluene under ambient conditions led to the isolation of monometallic aluminum complexes $[\text{ONE}^{\text{R}^1\text{R}^2}]_2\text{AlMe}$ (**1-3**) in 73-92% yield. Attempts to form $[\text{ONE}^{\text{R}^1\text{R}^2}]\text{AlMe}_2$ were not successful and **1-3** were even isolated from reactions of two equiv. AlMe_3 with 1 equiv. aminephenol. Treatment of Et_2AlCl with two equiv. of the corresponding ligand in toluene at ambient temperature afforded (**4-5**) in 86-90% yield. In this manner, two types of aluminum aminephenolate complexes were prepared where the labile group was either a methyl (**1-3**) or chloride ligand (**4-5**).



Scheme 1. Synthesis of methyl and chloro aluminum aminephenolate complexes

All complexes were isolated as colorless crystalline solids and were characterized by elemental analysis and ^1H , $^{13}\text{C}\{^1\text{H}\}$ and ^{27}Al NMR spectroscopy. The ^1H NMR spectra of **1-3** confirmed that the complexes were monometallic with two coordinated aminephenolate ligands. The methyl group in **1-3** gave rise to sharp signals upfield between 0.12 and -0.31 ppm. This signal was absent from the ^1H NMR spectra of **4-5** differentiating the alkyl complexes from those bearing chloride ligands. ^{27}Al NMR spectroscopy has been helpful in correlating chemical shift with coordination number and the ^{27}Al NMR shifts for compounds **1-5** (71-76 ppm, $w_{1/2} = 4010\text{-}3490$ Hz) fall within the range for five coordinate complexes.⁵⁴

Compounds **1-4** were characterized by single-crystal X-ray diffraction analysis and the crystallographic data are summarized in Table S8.⁵⁵ The τ (tau) value is a method of establishing the degree to which observed geometries for five coordinate compounds approaches either trigonal bipyramidal or square pyramidal geometry.⁵⁶ A value of zero describes a compound with perfectly square pyramidal parameters and a value of one is perfectly trigonal bipyramidal, while a value of 0.5 is intermediate between the two geometries. The τ values calculated for **1-4** are listed in Table 1. Compounds **1-3** are slightly distorted from trigonal bipyramidal, while compound **4** containing a chloride group possesses a near to perfect trigonal bipyramidal geometry. This slight difference between the methyl complexes (**1-3**) and chloro complex (**4**) might be attributed to steric differences between the alkyl and less bulky chloride groups within the Al coordination sphere.

Table 1. τ values for compounds **1-4**

Compound	τ value
$[\text{ONN}^{\text{Me,tBu}}]_2\text{AlMe}$ (1)	0.79
$[\text{ONN}^{\text{tBu,tBu}}]_2\text{AlMe}$ (2)	0.82

$[\text{ONO}^{\text{tBu,tBu}}]_2\text{AlMe}$ (3)	0.80
$[\text{ONN}^{\text{Me,tBu}}]_2\text{AlCl}$ (4)	0.97

The ORTEP plots of **1** and **2** are shown in Figure 2 and Figure S1 respectively and along with selected bond lengths and angles. Ligands are bound to the central metal in a bidentate manner with each of the methylamine groups orientated away from the Al center. This phenomenon was also observed in related zinc²⁷ and aluminum complexes.³⁹ The central nitrogen atoms of each ligand are bound to the Al center in the axial positions, with the equatorial sites occupied by the methyl group and two phenolate oxygen donors. These form two puckered six-membered rings (C_3NAIO). The bond angles around Al in **1** are O(1)-Al(1)-N(1), $90.33(5)^\circ$ and O(2)-Al(1)-N(1), $87.73(5)^\circ$ and the relative narrowness of the O(2)-Al(1)-N(1) bond angle can be attributed to the bite of the six-membered C_3NAIO chelate ring which possesses a torsion angle of $-15.9(2)^\circ$. This ring adopts a legless chair⁵⁷ conformation with N(1) and N(3) atoms forming the backrest and lie *ca.* 0.83 and 0.97 Å above the plane of Al-O(1)-C(1)-C(11)-C(12) and Al-O(2)-C(18)-C(28)-C(29) respectively. As expected, the two neutral nitrogen atoms occupying the axial sites exhibit longer contacts to the central Al (Al-N(1), 2.1612(14) Å and Al-N(3), 2.1567(14) Å) than the anionic equatorial contacts (Al(1)-C(35), 1.9901(18) Å, Al-O(1), 1.7898(12) Å and Al-O(2), 1.7911(12) Å). Al-O, Al-N and Al-C bond distances are comparable to related Al complexes reported elsewhere.⁵⁸⁻⁶⁰ The structural features of complex **2** are very similar to those in **1**, with the only significant difference being a more acute angle around the central Al atom [O(1)-Al-N(3)] in **2** than in **1**, possibly due to the greater steric demands of the *para* t-butyl group in **2** and resulting packing effects.

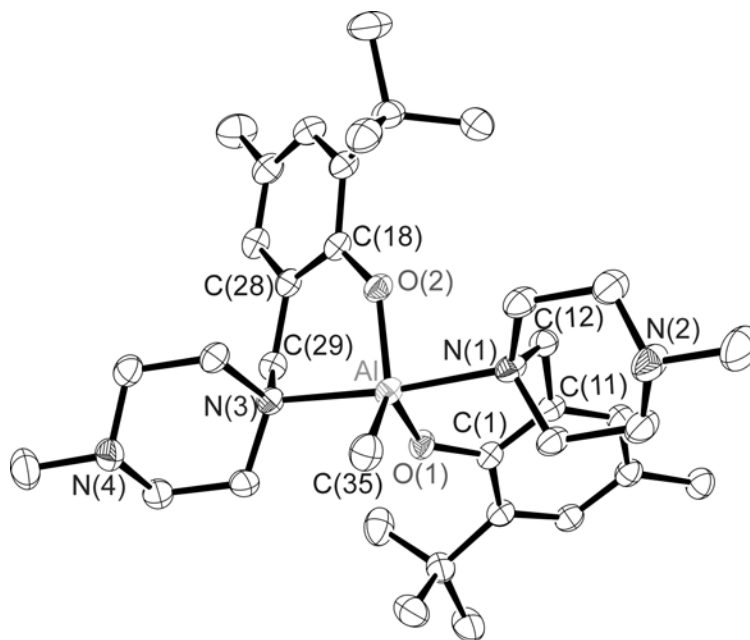


Figure 2. Molecular structure of **1**. (50% thermal ellipsoids; H atoms excluded for clarity). Selected bond lengths (Å) and bond angles (°): Al(1)-O(1), 1.7898(12); Al(1)-O(2), 1.7911(12); Al(1)-C(35), 1.9901(18); Al(1)-N(3), 2.1567(14); Al(1)-N(1), 2.1612(14); O(1)-C(1), 1.3597(17); O(2)-C(18), 1.3564(18); N(3)-C(29), 1.491(2); C(1)-C(11), 1.405(2); C(11)-C(12), 1.500(2); N(1)-C(12), 1.498(2); C(18)-C(28), 1.412(2); C(28)-C(29), 1.506(2) O(1)-Al(1)-O(2), 115.61(6); O(1)-Al(1)-C(35), 117.72(7); O(2)-Al(1)-C(35), 126.67(7); O(1)-Al(1)-N(3), 91.21(5); O(2)-Al(1)-N(3), 86.27(5); C(35)-Al(1)-N(3), 92.88(7); O(1)-Al(1)-N(1), 90.33(5); O(2)-Al(1)-N(1), 87.73(5); C(35)-Al(1)-N(1), 91.64(7); N(3)-Al(1)-N(1), 173.89(5); C(1)-O(1)-Al(1), 134.43(10); C(18)-O(2)-Al(1), 134.51(10)

Single crystal X-ray analysis shows that **3** crystallizes as a monometallic species in the orthorhombic space group *Pbca* and the ORTEP drawing is shown in Figure 3 along with selected bond lengths and angles. The structural features of **3** are similar to those of **1** and **2** with Al-N, Al-O and Al-C bond distances being within the range observed for **1**, **3** and other related complexes.⁵⁸⁻⁶⁰

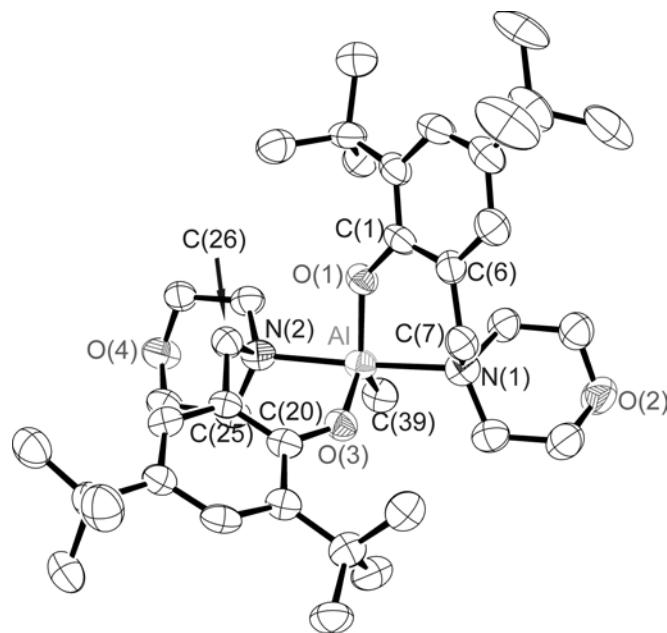


Figure 3. Molecular structure of **3**. (50% thermal ellipsoids; H atoms excluded for clarity). Selected bond lengths (Å) and bond angles(°): Al(1)-O(3), 1.792(4); Al(1)-O(1), 1.793(4); Al(1)-C(39), 1.981(7); Al(1)-N(2), 2.148(5); Al(1)-N(1), 2.151(5); O(1)-C(1), 1.350(7); N(2)-C(26), 1.489(8); N(2)-C(27), 1.499(8); O(3)-Al(1)-O(1), 117.1(2); O(3)-Al(1)-C(39), 118.2(3); O(1)-Al(1)-C(39), 124.6(3); O(3)-Al(1)-N(2), 88.6(2); O(1)-Al(1)-N(2), 88.9(2); C(39)-Al(1)-N(2), 93.6(3); O(3)-Al(1)-N(1), 88.6(2); O(1)-Al(1)-N(1), 86.7(2); C(39)-Al(1)-N(1), 93.4(3); N(2)-Al(1)-N(1), 173.0(2); C(30)-N(2)-Al(1), 110.9(4); C(26)-N(2)-Al(1), 103.1(4)

The ORTEP drawing of **4** is depicted in Figure 4, along with selected bonds lengths and angles. Complex **4** crystallizes in the monoclinic space group $C2/c$. The Al-O [1.7721(10) Å] and Al-N [2.1033(12) Å] bond distances are shorter than the corresponding bond lengths in **1-3** but longer than those of a related aluminum piperazinyl aminephenolate complex (η^2-N,O -[2-{CH₂N(C₄H₈NMe)}-6-PhC₆H₃O]AlMe₂), having Al(1)-O(1) [1.761(1) Å] and Al(1)-N(1) [2.045(1) Å].³⁹ The single crystal X-ray data for complex **5** were poor and could not be fully refined as a result of merohedral twinning. However, these data were sufficient to confirm gross connectivity and structural analogy to **4**.

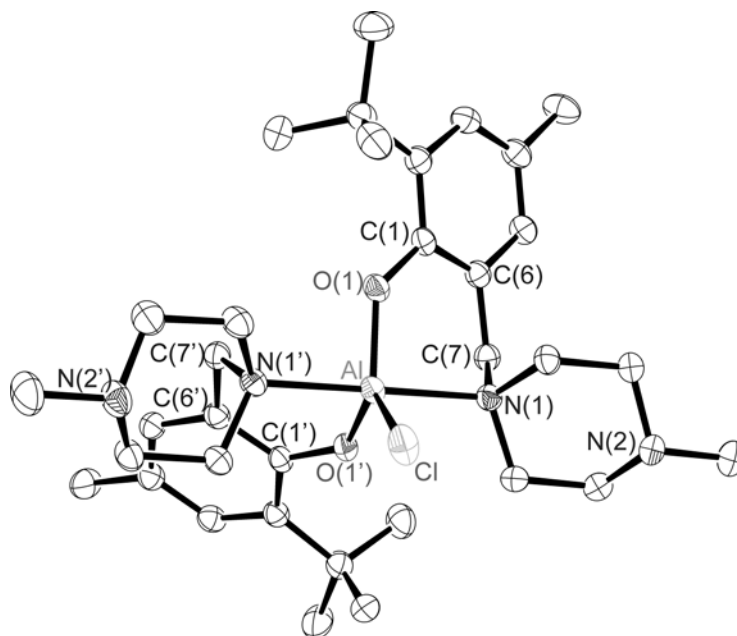


Figure 4. Molecular structure of **4**. (50% thermal ellipsoids; H atoms excluded for clarity). Selected bond lengths (Å) and bond angles (°): Cl(1)-Al(1), 2.2102(9); Al(1)-O(1), 1.7721(10); Al(1')-O(1'), 1.7721(10); Al(1)-N(1), 2.1033(12); O(1)-C(1), 1.3628(15); N(1)-C(7), 1.5031(16); O(1)-Al(1)-O(1'), 118.27(7); O(1)-Al(1)-N(1), 90.73(4); O(1)-Al(1)-N(1'), 89.61(4); N(1)-Al(1)-N(1'), 179.35(6); O(1)-Al(1)-Cl(1), 120.87(3); N(1)-Al(1)-Cl(1), 89.67(3).

Ring-opening polymerization of ϵ -caprolactone

Ring-opening polymerization (ROP) catalysis of ϵ -CL was carried out using **1-3** in the presence and absence of BnOH (results are summarized in Table 2). Complexes **1-3** showed low catalytic activity in the absence of BnOH with conversions of 16, 27 and 22% respectively at 80 °C within 30 minutes (Table 2; entries 1, 9 and 21) and so no further studies were conducted in this fashion. This contrasts with the good activity observed for related piperazinyl aminephenolate lithium complexes in the absence of alcohols, which yielded cyclic polymers in the ROP of ϵ -CL.¹⁰ **1-3** exhibit efficient catalytic activity in the polymerization of ϵ -CL in the presence of BnOH under the reaction conditions studied. The *in situ* formation of an alkoxide species under the reaction conditions employed was confirmed by ¹H NMR spectroscopy for the

1:1 reaction of complex **2** with BnOH (Figure S2). The signal of the methyl ligand disappeared and new resonances for the alkoxide group grew in. The formation of an alkoxide complex could also be seen in ^1H spectra from a 1:1 reaction of **4** with BnOH. *In situ* formation of active Al alkoxide complexes for ROP has been reported recently by Redshaw and co-workers for dialkylaluminum amidates⁶¹ and other authors for various metal complexes.⁶²⁻⁶⁴ The formation of an alkoxide species suggests that the mechanism of polymerization is via coordination-insertion and that an activated-monomer mechanism is less plausible.⁶⁵ However, in order to fully rule out the latter mechanism, further studies involving installation of less potent nucleophiles on the Al center would be required.⁴⁵ Polymerizations were relatively slow at room temperature 88, 96 and 78% monomer conversion were achieved in 150 minutes using **1**/BnOH, **2**/BnOH and **3**/BnOH respectively (Table 2, entries 3, 10 and 17), whereas similar conversions were obtained within 10 minutes at 80 °C. It should be noted that under identical conditions, **2**/BnOH did not facilitate ROP of *rac*-lactide (0% conv., 80 °C, 10 min). This is in stark contrast to the analogous Zn complex, EtZn**L2**, which in the presence of BnOH achieved quantitative conversion of *rac*-lactide at 70 °C after 90 min and measurable conversions after 10 minutes.²⁷ For ROP of ϵ -CL, it can be noticed that **2**/BnOH exhibits higher catalytic activity than **1**/BnOH and **3**/BnOH as it achieves higher conversions in a shorter time (Table 2, entries 7, 12, 19). However, **2**/BnOH produced polymers with lower molecular weights than those of **1**/BnOH, and the molecular weight distributions (M_w/M_n) of the polymers obtained using **1**/BnOH are narrower than those obtained using **2**/BnOH (Table 2, entries 2-8 and 10-16). This probably indicates that polymerization using **1**/BnOH is more controlled than that using **2**/BnOH. This is somewhat surprising given previous ROP reactions studied using Li and Zn complexes of these ligands,^{10,27}

where narrower M_w/M_n polymers were obtained from complexes bearing more sterically demanding ligands.

Table 2. Polymerization of ϵ -CL initiated by **1-5** in the presence and absence of BnOH^[a]

Entry	Initiator	[CL] ₀ /[Al] ₀ /[BnOH] ₀	t/min	T /°C	Conv (%) ^[b]	$M_{n,cal}^{[c]} \times 10^3$	$M_n^{[d]} \times 10^3$	$M_w/M_n^{[d]}$
1	1	50/1/0	30	80	16.0	—	—	—
2	1	75/1/1	12	80	73.8	6.31	5.17	1.30
3	1	100/1/1	150	25	82.2	9.35	8.18	1.34
4	1	100/1/1	10	80	78.2	8.93	6.46	1.31
5	1	150/1/1	10	80	69.9	11.9	9.08	1.34
6	1	200/1/1	18	80	92.1	21.0	15.4	1.65
7	1	100/1/1	35	60	84.6	9.58	7.77	1.33
8	1	100/1/1	55	40	87.0	9.93	7.82	1.42
9	2	50/1/0	30	80	27.0	—	—	—
10	2	100/1/1	150	25	96.7	10.9	8.62	1.65
11	2	100/1/1	10	80	97.6	11.0	5.14	2.51
12	2	100/1/1	12	60	88.9	10.1	5.47	1.51
13	2	100/1/1	24	40	79.3	9.01	5.80	1.59
14	2	75/1/1	12	80	98.8	8.38	3.88	2.19
15	2	150/1/1	12	80	99.1	16.9	9.71	1.89
16	2	200/1/1	10	80	96.1 ^e	21.9	15.3	1.76
17	3	100/1/1	150	25	78.8	8.90	4.12	1.69
18	3	100/1/1	54	40	54.8	6.16	4.96	1.47
19	3	100/1/1	24	60	83.4	9.47	5.91	1.42
20	3	100/1/1	12	80	95.9	10.8	5.70	1.96
21	3	50/1/0	30	80	22.3	—	—	—
22	3	75/1/1	12	80	91.0	7.79	4.49	1.88
23	3	150/1/1	10	80	89.0	15.2	8.54	2.23
24	3	200/1/1	10	80	88.0 ^f	20.0	14.3	1.91
25	4	100/1/1	12	80	83.0	9.47	6.27	1.30
26	4	100/1/0	24	80	92.9	10.6	12.3	1.73
27	4	100/1/0	30	60	50.5	5.76	52.7	2.4

28	5	100/1/0	10	80	41.1	4.69	10.3	1.99
29	5	100/1/0	14	60	28.1	3.20	13.5	2.21

[a] Reactions performed in toluene using the mole ratios, temperatures and reaction times indicated. [b] Determined by ^1H NMR spectroscopy. [c] The M_{ncal} value of the polymer was calculated with $M_{\text{ncal}} = ([\varepsilon\text{-CL}]_0/[\text{Al}]_0) \times 114.14 \times \text{conv. \%}$. [d] The M_n value was calculated according to $M_n = 0.56M_n^{\text{GPC}}$, where M_n^{GPC} was determined by GPC (chloroform), and is relative to polystyrene standards. [e] TOF 1150 h^{-1} . [f] 1050 h^{-1}

It was also observed that in all cases using **1-3**, the measured number average molecular weight of the polymers obtained via GPC were lower than the calculated values based on initial $[\text{Al}]:[\varepsilon\text{-CL}]$ ratios. This suggests that transesterification has occurred during the polymerization process. It is worth noting that the effect of $[\text{BnOH}]$ was investigated and it was found that an Al/BnOH molar ratio of 1:1 afforded the best activity whereas the presence of two or three equivalents of BnOH rendered the catalyst inactive. This observation is similar to that reported by Duda, wherein he used the aluminum isopropoxide trimer $[\text{Al}(\text{O}^i\text{Pr})_3]$ in the presence of diol $\{\text{HO}(\text{CH}_2)_5\text{OH}\}$ and suggested that the alcohol reversibly coordinated to the active species leading to catalytic inhibition.^{66,67}

In the polymerization reactions initiated by **4** and **5** in the absence of BnOH , gelation was observed for all reactions and conversion of $\varepsilon\text{-CL}$ did not reach completion in 5.00 mL of toluene, the volume used in ROP using **1-3**/ BnOH above, due to increased viscosity resulting from a rapid increase in molecular weight. However, in 10.00 mL of toluene the polymerization could proceed, albeit not to completion (Table 2; entries 26-29). For these reactions, the molecular weight data obtained by GPC for each of the polymerization runs were much higher than calculated theoretical values, while the molecular weight distributions (M_w/M_n) were rather broad. Zhang *et al.*^{68,69} reported similar observations with aluminum complexes of functionalized phenolate ligands, which he interpreted to arise from higher reaction temperatures resulting in transesterification.⁷⁰⁻⁷² However, it could also be that when **4** and **5** are used, initiation proceeds

via acid-initiation (HCl generated *in situ* from adventitious water) and this reaction is more uncontrolled than in reactions catalyzed by an Al-alkyl/alcohol system. Another possibility is that the reaction may be proceeding via a reaction pathway involving insertion of the monomer into the Al-Cl bond. This has previously been suggested as a plausible mechanism for ROP of trimethylene carbonate using a chloro-aluminum salen complex.⁷³ Due to the broad polydispersity of the polymer produced using **4** and **5** without BnOH, the polymerization mechanism for these systems was not studied in detail. The resulting polymers were characterized using ¹H NMR spectroscopy and MALDI-TOF MS, as discussed below. No alkoxide end groups are seen in polymers that were isolated from reactions using **4** or **5** when no BnOH was used as co-initiator. It should be noted that 1.0 M anhydrous HCl in ether has previously been reported to facilitate ROP of ϵ -CL to yield high molecular weight, polydisperse polymer,⁷⁴ and that under reaction conditions similar to those reported in this study using Al complexes, 16.7 mM HCl in toluene afforded 43% conversion of ϵ -CL at 80 °C in 15 min. Therefore, at this stage, both an acid catalyzed reaction and insertion of the monomer into the Al-Cl bond remain plausible mechanisms.

Polymers obtained using complexes **1-5** in the presence or absence of BnOH were characterized using GPC, MALDI-TOF MS, ¹H NMR spectroscopy, TGA and DSC. Discussion of the TGA and DSC data can be found in supporting information.

End group analysis by ¹H NMR spectroscopy and MALDI-TOF mass spectrometry

A ¹H NMR spectrum of a typical polymer sample obtained using **1-3** is shown in Figure 5. Methylene proton signals were assigned at 1.38, 1.65, 2.31 and 4.06 ppm. The presence of aromatic benzyl protons at 7.35 ppm, and the benzyl and hydroxyl methylene signals at 5.12 and

3.65 ppm with an integral ratio close to 1 indicate the formation of linear polymers capped with a benzyloxy group at one end and a hydroxyl group at the other. $^{13}\text{C}\{^1\text{H}\}$ NMR analysis confirmed end-group assignments with resonances of CH_2OH and OCH_2Ph appearing at 62.58, 66.15 and 128.55 ppm respectively (Figure S4). These signal assignments are in good agreement with results reported previously.⁷⁵ This observation is consistent with acyl-oxygen bond cleavage of $\epsilon\text{-CL}$, which would occur in ROP reactions occurring via either a coordination-insertion or activated monomer mechanism.

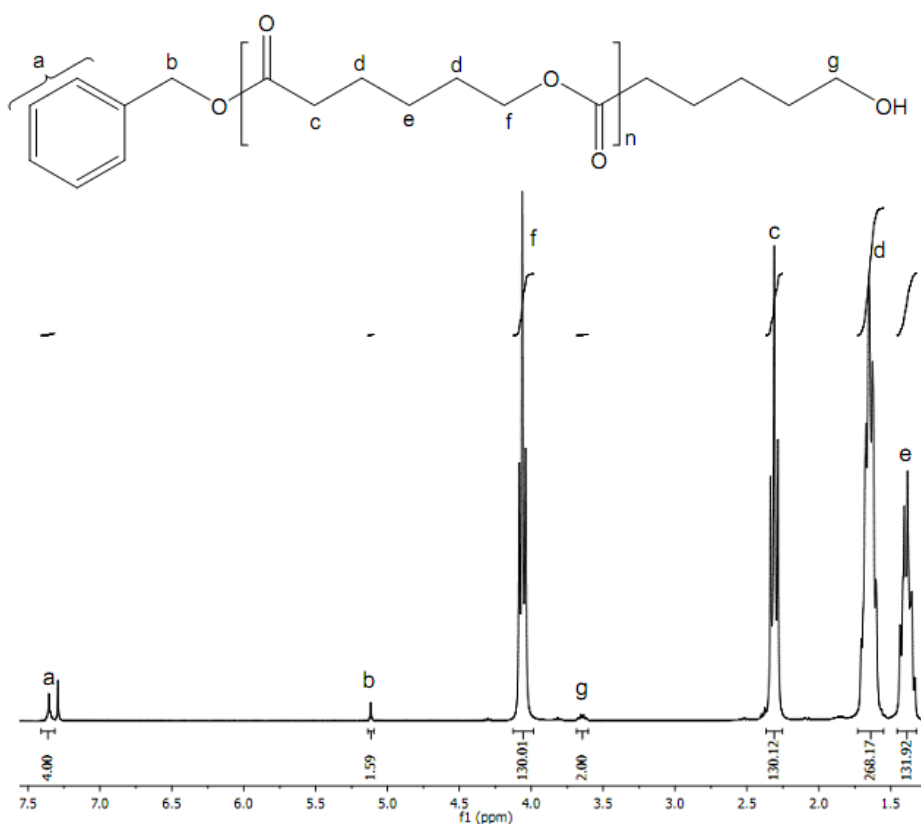


Figure 5. Typical ^1H NMR spectrum of PCL prepared using **1-BnOH** (Table 2, entry 7)

The ^1H NMR spectrum (Figure S5) of the polymers obtained with chloride complex **4** indicates that the polymer is a linear chain, evidenced by the resonance at 3.67 ppm, which corresponds to the terminal methylene proton (CH_2OH). However, no other assignable end-

group resonances were located and as a result, information about the initiating group and the mechanism could not be obtained from ^1H NMR spectroscopy. However, it is clear that insertion in the Al-phenolate bond is not occurring.

Further end-group analyses were conducted through MALDI-TOF mass spectrometry. The mass spectrum of the polymer prepared with **2**/BnOH is depicted in Figure 7 (Table 2, entry 11) and revealed the presence of a single major peak series. Further mass spectra are available in supporting information. Each successive group of peaks exhibits a mass difference of 114 Da corresponding to the repeating unit of ϵ -caprolactone and is in agreement with polycaprolactone chains capped with benzyloxy groups clustered with sodium ions to give adducts: $(\text{BnO}\{\text{CL}\}_n\text{H})+\text{Na}$ [e.g. $n = 11$, m/z 1385.3376 (exp.), 1385.80 (calc.)]. In addition to the major peak population, minor sets of peaks at the low m/z region of the spectrum (inset) could be attributed to macromolecules associated with potassium ions rather than sodium [e.g. $n = 11$, m/z 1401.7856 (exp.), 1401.77(calc.)], similar to results observed by Mata *et al.*⁶² A second minor set of peaks, differing by 15 mass units from the first minor series, might possibly be assigned to a protonated methyl terminated polymer associated with potassium ions, $(\text{BnO}\{\text{Cl}\}_n\text{CH}_3)+\text{H}+\text{K}$ [e.g. $n = 11$, m/z 1416.9983 (exp.), 1416.79 (calc.)]. This minor series of peaks did not fit models for other possibilities including incorporation of the ligand and association with other metal ions including aluminum. How the methyl group proposed has been incorporated into or become associated with the polymer is not clear at this stage, especially as resonances for such a group were not observed in the ^1H NMR spectra of the polymer. It should be noted that MALDI-TOF MS is a more sensitive technique for detecting impurities and differences in end groups for polyesters than ^1H NMR and that reactions can also occur in the spectrometer leading to polymer modification.⁷⁶ The identification of PCL capped with benzyloxy and hydroxy end-groups as the

main signals in the MALDI-TOF mass spectrum is in agreement with ^1H NMR analysis. There is little evidence for transesterification side reactions (either intra- or intermolecular) occurring from the mass spectra of this polymer, despite the lower than expected molecular weights indicated by GPC data.

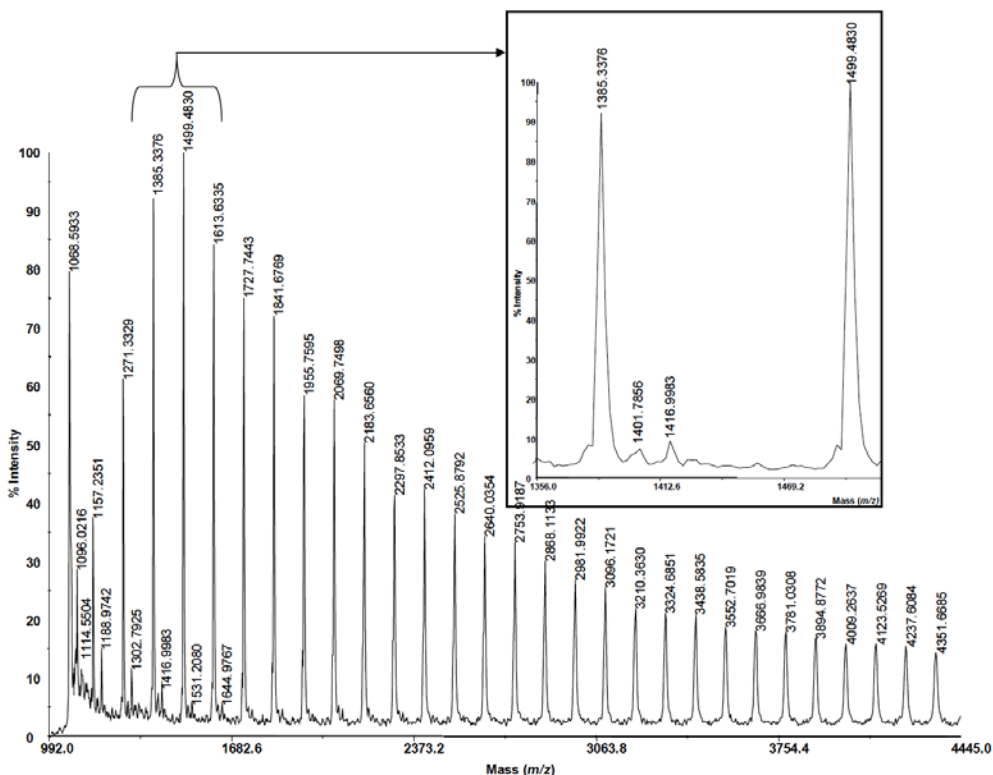


Figure 7. MALDI-TOF mass spectrum of PCL initiated by **2**-BnOH in toluene at 80 °C, $[\text{CL}]/[\text{2-BnOH}] = 100$ (Table 2, entry 11).

The MALDI-TOF spectrum of PCL obtained using **4** as initiator (Figure S8) displays two sets of peak distributions. The major series of peaks (the most important) correspond to macromolecules capped on each end with chloride and hydroxyl groups ($\text{Cl}\{\text{CL}\}_n\text{OH}$) [e.g. $n = 12$, m/z 1420.69 (exp.), 1420.79 (calc.)]. The remaining minor series of peaks were assigned to macromolecules capped with hydroxyl groups, ($\text{H}\{\text{CL}\}_n\text{OH}$) [e.g. $n = 12$, m/z 1387.1106 (exp.),

1386.83 (calc.)]. Similar hydroxyl terminated macromolecules have been previously reported by others.^{62,77} The main chlorinated polymer product could be formed from either monomer insertion into the Al-Cl bond or initiation by HCl.

Kinetic studies of ϵ -CL polymerization

In order to better understand the nature of ϵ -caprolactone polymerization initiated by **1-3** in the presence of BnOH, a series of polymerization reactions were conducted in toluene at 80 °C for various monomer to initiator [CL]/[Al] mole ratios to determine the effect of [CL] and [Al] on the catalytic activity. The conversion of ϵ -caprolactone was monitored by ¹H NMR spectroscopy and semilogarithmic plots of $\ln[\text{CL}]_0/[\text{CL}]_t$ versus time for the polymerizations initiated by **2**/BnOH are shown in Figure 8 (Plots for **1**/BnOH and **3**/BnOH are shown in supporting information, Figure S11 and S12). These plots revealed that reaction rates slightly decreased with increasing [CL]/[Al] molar ratio in all cases investigated. In addition, it was observed that number average molecular weight M_n obtained by GPC increased linearly as monomer to initiator ratios [CL]/[Al] were increased as shown in Figure 9 (Figure S13 and S14) which demonstrates the “living character” of the polymerization process, implying that the growing polymer chain does not terminate as the polymerization progresses. Similar results have been previously reported by Wu and co-workers⁷⁸ and others for bridged bulky aluminum phenoxide initiator systems.^{79,80} However, it should also be noted that in the current study at higher ϵ -CL:Al ratios there is some deviation from this linearity towards formation of higher M_n polymer that potentially indicates occurrence of termination by chain-transfer under such conditions.

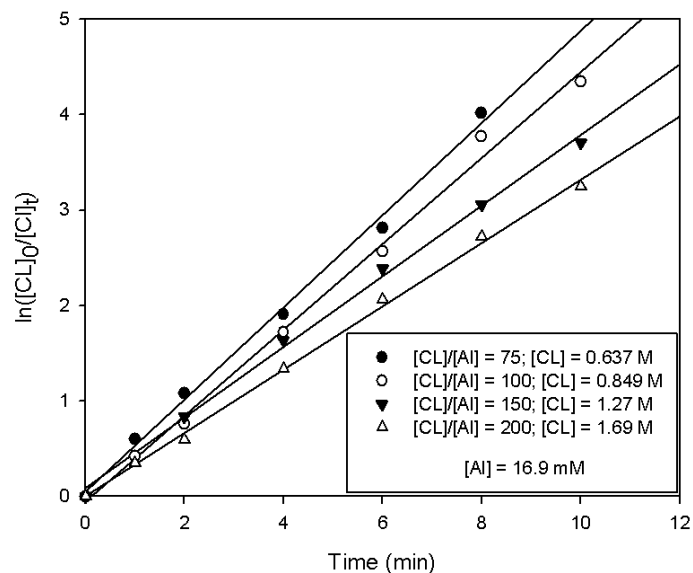


Figure 8. Semilogarithmic plots of the monomer conversion stated as $\ln[\text{CL}]_0/[\text{CL}]_t$ versus the reaction time for the polymerization of ϵ -caprolactone at different monomer molar ratios initiated with (a) **2**; $[\text{CL}]_0/[\text{2-BnOH}]_0 = 75$ (●), 100 (○), 150 (▼), 200 (▲), ($[\text{2}]_0 = 16.9$ mM, 80 °C)

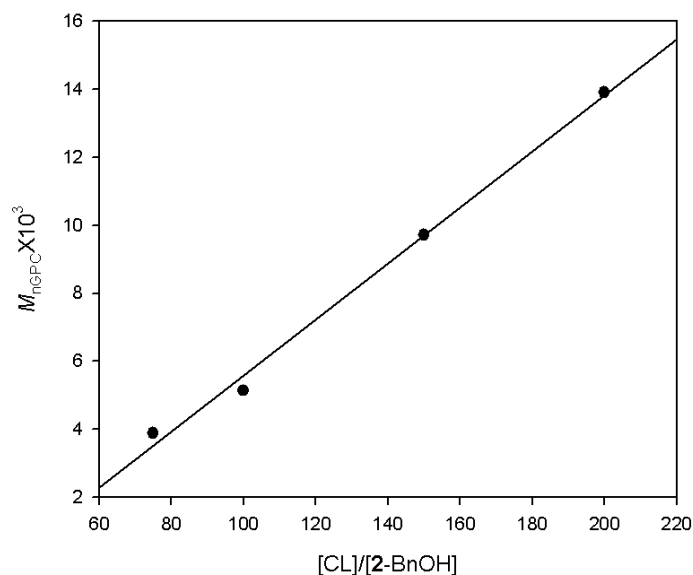


Figure 9. Relationship between $M_{n,\text{GPC}}$ of the polymer and the initial mole ratio $[\text{CL}]_0/[\text{2-BnOH}]$ for the polymerization of ϵ -CL initiated by **2**-BnOH in toluene at 80 °C. $R = 0.9974$, $R^2 = 0.9948$.

By conducting the reactions over a range of temperatures, it was observed that the overall polymerization rate (k_{obs}) increases with an increase in temperature as shown in Figure 10 (and

supporting information Figures S15 and S16). The semilogarithmic plots shown herein are linear, indicating a first-order dependence of reaction rate with respect to monomer concentration and pass through the origin indicating the absence of an induction period,^{81,82} which is in contrast to some previous polymerization reactions using aluminum alkoxides where induction periods were observed.^{75,83} This might also imply that the reaction is proceeding via an activated monomer mechanism but it might also be an artifact of the temperatures at which reactions were studied. Greater linearity can be seen in the plots for reactions conducted at higher temperatures, where a shorter induction period would also be expected. It should be noted that the aluminum complex and BnOH were mixed and heated alone to the reaction temperature (to allow the active alkoxide species to form) before mixing with the preheated monomer solution.

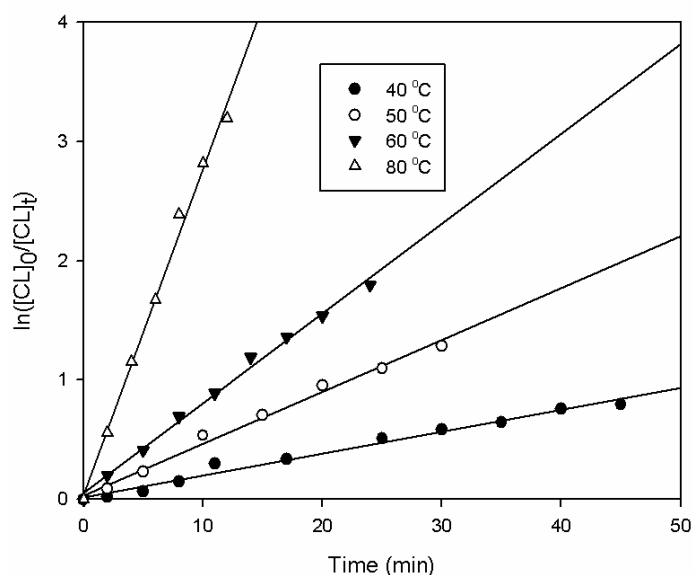


Figure 10. Semilogarithmic plots of the monomer conversion stated as $\ln[CL]_0/[CL]_t$ versus the reaction time for the polymerization of ϵ -caprolactone at different temperatures initiated with 3-BnOH; $[CL]_0/[3\text{-BnOH}]_0 = 100$, ($[3\text{-BnOH}]_0 = 16.9$ mM, $[CL] = 0.845$ M); (●) = 40 °C, (○) = 50 °C, (▼) = 60 °C, (△) = 80 °C.

The observed rate constant (k_{obs}) for each catalyst was obtained from the slope of $\ln[CL]_0/[CL]_t$ versus time and are summarized in Table 3. It can be seen that the fastest

polymerization was observed for **2**/BnOH. In comparison, the value determined for **2**/BnOH is about twice that of **1**/BnOH and only slightly higher than that of **3**/BnOH under similar reaction conditions, i.e. the rate of polymerization by **1-3** in the presence of BnOH follows the order $\mathbf{2/BnOH} \geq \mathbf{3/BnOH} > \mathbf{1/BnOH}$. For further clarification, comparative semilogarithmic plots obtained for the polymerization of ϵ -CL by **1-3** in the presence of BnOH are provided in the supporting information (Figure S17). We therefore hypothesize that the more bulky *tert*-butyl substituent in the *para* position of the ligand has some influence on the catalytic behavior of the complexes despite being somewhat remote from the center of reactivity. This observation is similar to that reported by Chmura *et al.*⁸⁴ for Ti(IV) complexes of bis(phenolate)s, but in contrast to the aluminum systems reported by other authors where less sterically demanding ligands afforded more effective initiators.^{85,86} However, by comparing the activity of the methyl complexes with the chloride complexes, the latter showed lower activity and produced polymers with different properties. This trend has also been observed by others.⁵⁰ To draw comparisons to previously reported kinetic data for other initiators, some rate constant values are collected in Table 3. The values determined for **1** and **2** in the presence of BnOH are similar to the values observed by us for the piperazinyl aminophenolate lithium complexes with the same supporting ligand under similar reaction conditions but lower temperature.¹⁰ The k_{obs} values for **1-3**/BnOH are significantly lower than that of diethylaluminum ethoxide⁸⁷ but higher than those for some other aluminum alkoxides albeit at lower temperatures.^{88,89} Reaction rates obtained using analogous Zn complexes containing **L1** and **L3** are significantly lower than those obtained using the corresponding Al compounds.²⁷ This contrasts with the increased reactivity observed using the Zn complexes of the same ligands compared with Al derivatives in ROP of *rac*-LA. This implies that the choice of monomer has a significant influence on the relative reactivity of

catalysts and this should be taken into account when designing new systems for ROP of cyclic esters. The Al complexes contain two ligands per metal center and this leads to a more sterically congested reaction site compared with the Zn compounds that contain only one amine-phenolate ligand per Zn. In ROP, *rac*-LA can be considered a more sterically demanding monomer than ϵ -CL. The methyl groups within the monomer and growing polymer chain would interact unfavorably with ligands that potentially block the binding site for incoming monomer. In contrast, ϵ -CL polymerization is perhaps affected more strongly by the Lewis acidity of the metal center (electronics rather than sterics) and therefore, the Al complexes are more reactive than their Zn analogs.

The relationship between $\ln k_{\text{obs}}$ and the reciprocal of polymerization temperature ($1/T$) is shown in Figure 11 (Figure S18 and S19). According to the Arrhenius equation, the activation energies calculated for **1**/BnOH, **2**/BnOH and **3**/BnOH are shown in Table 4.

Table 3. A comparison of rate constants for ϵ -caprolactone polymerization initiated by various metal complexes in toluene.

Entry	Initiator	T /°C	k_{obs} (Lmol ⁻¹ min ⁻¹)	Ref
1	Et ₂ AlOCH ₂ CH ₃	25	8.40	87
2	Al[O(CH ₂) ₃ NEt ₂] ₃	25	3.00	88
3	Et ₂ AlO(CH ₂) ₃ NEt ₂	25	0.030	88
4	Et ₂ AlO(CH ₂) ₃ CH=CH ₂	25	0.160	88
5	Me ₂ Al[O-2- ^t Bu-6{(C ₆ F ₅)N=CH}C ₆ H ₄]/BnOH	50	0.028	89
6	{Li[ONN ^{Me,tBu}]} / BnOH	40	0.133	10
7	{[ONN ^{Me,tBu}] ₂ AlMe} (1/BnOH)	80	0.153 ^a 0.129 ^b	This work
8	{[ONN ^{tBu,tBu}] ₂ AlMe} (2/BnOH)	80	0.371 ^a	This work
9	{[ONO ^{tBu,tBu}] ₂ AlMe} (3/BnOH)	80	0.274 ^a 0.221 ^c	This work
10	{[ONN ^{Me,tBu}] ₂ ZnEt} / BnOH	70	0.047 ^d	27
11	{[ONO ^{tBu,tBu}] ₂ ZnEt} / BnOH	70	0.072 ^e	27

^a [CL]/[Al] = 100, [Al] = 16.9 mM. ^b [CL]/[Al] = 150, [Al] = 16.9 mM. ^c [CL]/[Al] = 200, [Al] = 16.9 mM. ^d [CL]/[Al] = 200, [Al] = 22.5 mM. ^e [CL]/[Al] = 200, [Al] = 18.8 mM

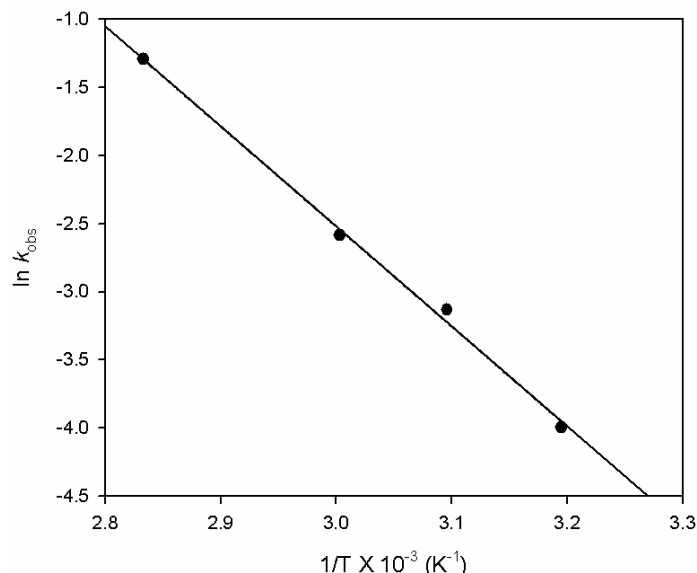


Figure 11. Arrhenius plot of $\ln(k_{obs})$ vs. $1/T$ for ROP of ϵ -caprolactone initiated by **3**/BnOH: $[\mathbf{3}/\text{BnOH}] = 16.9 \text{ mM}$; $[\text{CL}]/[\mathbf{3}/\text{BnOH}] = 100$. $R = 0.9984$, $R^2 = 0.9968$.

The activation energy for **3** is higher than those of **1** and **2** and this must be attributed to the difference in outersphere (E) substituents within the complexes. It is possible that the methylamine (NMe) group of **1** and **2**, which is a stronger base than the ether (O) group of **3**, activates the incoming monomer via non-covalent interactions. Another explanation could be that when $E = \text{O}$ (**3**) the ether donor can coordinate temporarily with the Al center and block the vacant coordination site from incoming monomer. In contrast, when $E = \text{NMe}$ (**1** and **2**) the nitrogen would need to undergo inversion to coordinate to the metal center and therefore, the coordination site for incoming monomer remains accessible. The activation energy values obtained for **1**/BnOH and **2**/BnOH were similar to those reported for $\text{Et}_2\text{AlO}(\text{CH}_2)_3\text{CH}=\text{CH}_2$, while the value for **3**/BnOH is similar to those given for $\text{Et}_2\text{AlO}(\text{CH}_2)_3\text{NET}_2$.⁸⁸ It is worth noting that this last literature example also contains an amine group within the coordination sphere of the metal and although opposite to the trend we observe, this further indicates that outersphere heteroatoms can influence activation energies in ROP reactions. For the piperazinyll

aminephenolate lithium complex/BnOH with the same supporting ligand as **1**/BnOH,¹⁰ a higher activation energy was measured compared with the aluminum system. This possibly indicates that the monomer is more activated in the current system compared with the analogous lithium one. Furthermore, more controlled ROP was demonstrated by the piperazinyl aminephenolate aluminum complexes and this might be due to less opportunity for competing side reactions in the aluminum-catalyzed process due to the presence of two ligands per metal center rather than one. In reactions using the lithium complexes, ROP could be initiated by the phenolate nucleophile in addition to the alkoxide,¹⁰ whereas no evidence for this has been seen with the aluminum species discussed herein.

Table 4. A comparison of activation energy (E_a) for ϵ -caprolactone polymerization initiated by various aluminum and metal complexes

Initiator	E_a (kJ mol ⁻¹)	Ref
{[ONN ^{Me,tBu}] ₂ AlMe}(1 /BnOH)	39.7	This work
{[ONN ^{tBu,tBu}] ₂ AlMe}(2 /BnOH)	31.8	This work
{[ONO ^{tBu,tBu}] ₂ AlMe}(3 /BnOH)	61.0	This work
{Li[ONN ^{Me,tBu}]} / BnOH	53.4	10
Et ₂ AlO(CH ₂) ₃ CH=CH ₂	42.3	88
Et ₂ AlO(CH ₂) ₃ NEt ₂	57.3	88

The kinetic data were also subjected to Eyring analyses (Table 5, Figures S20-S22). This shows that in terms of both enthalpy and entropy there are significant differences between **1**/BnOH and **2**/BnOH compared with **3**/BnOH. However, the free energies of activation at 80 °C are all very similar (~ 90 kJmol⁻¹) and comparable with a value recently reported for an Al half-salen complex for ROP of ϵ -CL (95 kJmol⁻¹, 90 °C).⁹⁰ Computational studies are needed in order to

determine the reasons behind the significant differences in the entropic and enthalpic components for the systems reported in the current study.

Table 5. A comparison of activation parameters for ϵ -caprolactone polymerization initiated by aluminum complexes **1-3**.

Initiator	$\Delta H^\ddagger/\text{kJmol}^{-1}$	$\Delta S^\ddagger/\text{Jmol}^{-1}\text{K}^{-1}$	$\Delta G^\ddagger/\text{kJmol}^{-1}$ ^a
1 /BnOH	36.9(\pm 0.7)	-150(\pm 1)	90
2 /BnOH	29.0(\pm 0.1)	-180(\pm 1)	93
3 /BnOH	58.2(\pm 0.2)	-92(\pm 1)	90

[a] T = 80 °C

Copolymerization of carbon dioxide and epoxides using **4** and **5**

Compound **5** with PPnCl (bis(triphenylphosphoranylidene)ammonium chloride) as co-catalyst was preliminarily screened for the reaction of styrene oxide (SO) and CO₂. The results are summarized in Table 6, in which very low conversion to styrene carbonate (SC) was obtained with the combination of **5** and PPnCl for 3 h (Table 6, entry 1). However, when the time was increased to 24 h, the conversion improved about three fold (Table 6, entry 2). A control reaction using the co-catalyst alone was conducted and the activity was slightly less than that in the presence of **5** under similar reaction conditions (Table 6, entry 3). The observed decrease in activity confirms that **5** is a catalyst for the coupling reaction, albeit with low activity.

Table 6. Coupling reactions of SO and CO₂ using **5** and PPnCl^a

Entry	Catalyst	Co-catalyst	$[\text{SO}]_0/[\text{Al}]_0/$ $[\text{Co-cat}]_0$	t (h)	P [CO ₂] (bar)	T (°C)	SC conv. (%)
1	5	PPnCl	200/1/1	3	40	60	9.3
2	5	PPnCl	200/1/1	24	40	60	37.0
3	–	PPnCl	200/0/1	24	40	60	23.7

^aPPnCl = bis(triphenylphosphoranylidene)ammonium chloride

Table 7 contains data from attempted CHO/CO₂ copolymerization reactions using compounds **1**, **4** and **5** as catalysts. In all cases a [CHO]:[Al] ratio of 500:1 was used and 40 bar CO₂ unless otherwise indicated. It should be noted that in none of the reactions described here was polyether formation observed. This contrasts with related cationic Al complexes, which show good activity in ROP of epoxides.^{39,91} Compound **1** with tetrabutylammonium fluoride (Bu₄NF) was found to couple cyclohexene oxide (CHO) and CO₂ in neat CHO at 80 °C (Table 7, entry 1). Cyclohexene carbonate (CHC) at 38 % conversion levels was detected with 97% *cis* stereoselectivity. Reactions of CHO and CO₂ using compound **4** showed that it was inactive towards both copolymerization and cycloaddition reactions even in combination with PPnCl as a co-catalyst (Table 7, entries 2 and 3). Compound **5** was found to be active without a co-catalyst producing a copolymer (Table 7, entry 4). The resulting polymer was a polyethercarbonate, which consists of polyether (m) and polycarbonate (n) with 54% carbonate linkages. Both the polyether and polycarbonate portions were identified and quantified through ¹H NMR spectroscopy using the signal of methine hydrogen atoms as shown in the supporting information (Figure S23). Efforts to enhance the activity of **5** were attempted by adding PPnCl as a co-catalyst. However, this led to inactivity of **5**, possibly by the co-catalyst blocking the active site hindering monomer access to the metal center. These preliminary results also demonstrate significant differences between **4** and **5**, which are probably due to the nature of the outer-sphere heteroatom. We propose that **5** is better able than **4** to support the formation of an ionic complex, where the chloride is not closely associated with the aluminum center, Figure 13. The nucleophilic chloride ion would then be able to ring-open the epoxide, which could be bound to the aluminum center. We suggest that chloride ion dissociates more readily from the aluminum center in **5** because the metal can more readily coordinate the formally outer-sphere ethereal

donor atom compared with the amine donor atom in **4**. The morpholinyl-oxygen in **5** possesses two lone pairs, is less sterically demanding and the morpholinyl-ring potentially undergoes conformational changes with less energy compared with the piperazinyl-ring in **4**. Coordination of the nitrogen atom in **4** to the aluminum center in order to stabilize the ionic form of the complex would require stereochemical inversion of the nitrogen center. These initial results in the area of carbon dioxide activation are promising but further reaction optimization is required for **5** to be competitive with other copolymerization catalysts,^{92,93} and computational studies are needed in order to understand the difference in reactivity compared with **4**.

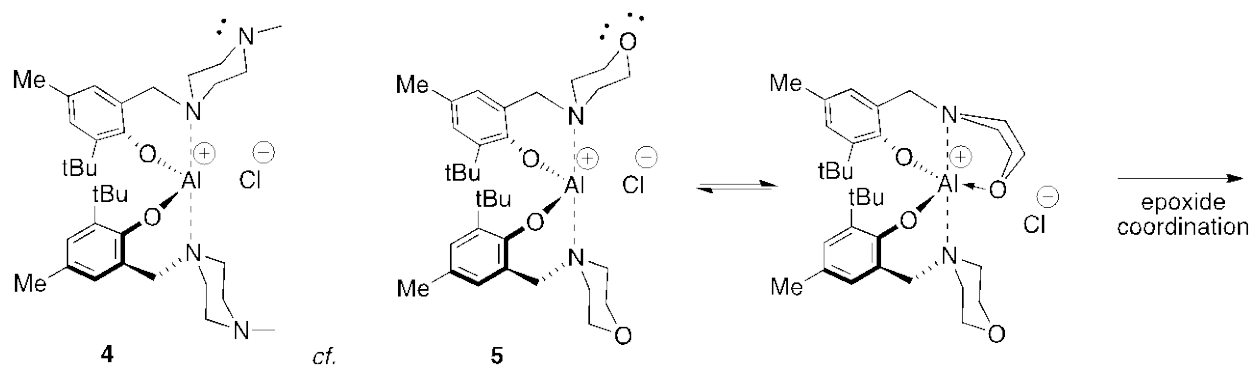


Figure 12. Possible key ionic intermediate in CO₂-epoxide copolymerization facilitated by **5**.

Table 7. Copolymerization of CHO/CO₂ using **1**, **4** and **5** as catalysts^a

Entry	Cat.	Co-cat.	[Al] ₀ / [Co-cat] ₀	t (h)	% CHC ^b	% Polymer ^b [% Carbonate]	M _n ^c (kg/mol)	M _w /M _n ^c
1 ^d	1	Bu ₄ NF	1/1	24	38.3 (97.0% <i>cis</i>)	0	—	—
2	4	—	1/0	24	0	0	—	—
3	4	PPNCl	1/1	24	0	0	—	—
4	5	—	1/0	16	0	66.7 [54.0]	29.0	3.16
5	5	PPNCl	1/1	24	0	0	—	—

^a Reactions run neat at 60 °C with [CHO]:[Al] 500:1, CO₂ pressure of 40 bar. PPNCl = bis(triphenylphosphoranylidene)ammonium ^b Determined by ¹H NMR. ^c Determined by GPC calibrated with polystyrene standards in chloroform. ^d Run neat at 80 °C and CO₂ pressure of 65 bar.

Conclusions

In summary, aluminum alkyl and halide complexes supported by monoanionic piperazinyl- and morpholinyl-aminephenolate ligands were synthesized and fully characterized. Aluminum alkyl complexes **1-3** are efficient catalysts for the ROP of ϵ -CL in the presence of BnOH, and possess good activity (TOF $\sim 1000 \text{ h}^{-1}$, $80 \text{ }^\circ\text{C}$) for this reaction based on the reactivity scale developed by Redshaw and Arbaoui.⁴ In comparison with previously reported Zn analogs,²⁷ the Al complexes exhibit higher reactivity in ROP of ϵ -CL but lower (zero) reactivity in ROP of *rac*-LA. This study sheds some light on ways to develop active catalysts for ROP of lactones and demonstrates that significant differences in reactivity trends occur when studying different monomers. Based on the experimental data, the reactivity of the complexes has the order **2**/BnOH \geq **3**/BnOH $>$ **1**/BnOH. Polymerization kinetic studies revealed a first order dependence on monomer concentration. Comparison of the activation energies of polymerization for piperazinyl-aminephenolate and morpholinyl-aminephenolate complexes revealed that the activation energy is lower for the piperazinyl-containing complexes than for the morpholinyl-containing complex, highlighting the effects of the outersphere (E) substituent groups on the resulting activity of complexes in ROP reactions. Differences were noted between the activation entropies and enthalpies for the reactions using these complexes. However, the free energies of activation for all three complexes were similar. **4** ($\{[\text{ONN}^{\text{tBu,tBu}}]_2\text{AlCl}\}$) was not active in CHO/CO₂ copolymerization, in contrast, **5** ($[\text{ONO}^{\text{tBu,tBu}}]_2\text{AlCl}$) was active even without a co-catalyst. This shows that the E substituent once again impacted the activity of these complexes within a reaction. We propose that this is due to facile coordination of the ethereal morpholinyl oxygen atom to the metal center, which displaces the chloride ion which can then ring-open the

epoxide. Further studies are required to understand the subtle differences in reactivity observed and build on these discoveries particularly with regards to carbon dioxide copolymerization.

Experimental Section

All experiments involving metal complexes were performed under a nitrogen atmosphere using standard Schlenk and glove-box techniques. Toluene, hexane and pentane were purified using an MBraun Solvent Purification System. Deuterated solvents (C_6D_6 , $CDCl_3$, C_5D_5N , C_7D_8) were purchased from Cambridge Isotope Laboratories, Inc., purified and dried before use. All solvents were degassed using freeze-pump-thaw cycles prior to use. 2,4-di(*tert*-butyl)phenol, 2-*tert*-butyl-4-methylphenol, 1-methyl piperazine, morpholine, trimethylaluminum (25% w/w in hexane), diethylaluminum chloride (25% w/w in heptane), and ϵ -caprolactone were purchased from Sigma-Aldrich or Alfa Aesar. ϵ -Caprolactone was dried and degassed prior to use. Cyclohexene oxide (CHO) was refluxed over CaH_2 , distilled and stored under nitrogen. CO_2 (99.99% purity) was used without further purification. Elemental analyses were performed by Canadian Microanalytical Service Ltd., Delta, BC, Canada. 1H and $^{13}C\{^1H\}$ NMR spectra were recorded on a Bruker Avance 300 or 500 MHz spectrometer at 25 °C (unless otherwise stated) and were referenced internally using residual proton and ^{13}C resonances of the solvent. ^{27}Al NMR spectra were recorded on a Bruker 300 MHz spectrometer and referenced externally to $Al_2(SO_4)_3$ in D_2O . For polymer MALDI-TOF MS analysis, an Applied Biosystems 4800 TOF-TOF instrument was used and the mass spectra were recorded in linear mode. 2-(4-hydroxyphenylazo)benzoic acid (HABA) was used as the matrix and purified tetrahydrofuran was used as the solvent for depositing analytes onto the instrument plate. Mass spectra were modeled using mMass software (www.mmass.org). GPC data were collected on a Viscotek

GPCMax system equipped with a refractive index detector and columns purchased from Phenomenex (Phenogel 5 μ Linear/mixed bed 300 \times 4.60 mm column). Samples were run in chloroform at 35 $^{\circ}$ C at a concentration of 1 mg/mL. The instrument was calibrated against polystyrene standards (Viscotek) to determine the molecular weights (M_n and M_w) and the polydispersity index (M_w/M_n) of polymers. Conversions were determined by ^1H NMR integration of the ϵ -methylene of residual ϵ -caprolactone and poly(ϵ -caprolactone). TGA measurements were obtained using a TGA Q500 Thermogravimetric Analyzer (TA Instruments). Approximately 4.8 mg of sample was loaded onto the open platinum pan. The samples were heated from 25 to 600 $^{\circ}$ C under dry nitrogen at a constant heating rate of 50 $^{\circ}$ C/min using the high-resolution method (dynamic rate). The TGA data were plotted as temperature versus weight %, from which onset and final decomposition temperatures were obtained. Data were also plotted as temperature versus derivative of weight %, from which peak decomposition temperatures were obtained. Melting temperatures of PCL samples were obtained using a DSC1 STAR^e System (Mettler Toledo). The measurements were carried out at a scanning rate of 10 $^{\circ}$ C/min and nitrogen gas flow rate of 50 ml/min with approximately 4.0 mg of sample. Samples were heated from -70 to +150 $^{\circ}$ C and the melting point was determined at the maximum of the melting endotherm.

Single Crystal X-ray Diffraction Studies

Crystals of **1-4**, and **5** (Figure S1) were mounted on low temperature diffraction loops and measured on a Rigaku Saturn CCD area detector with graphite monochromated Mo-K α radiation. Structures were solved by direct methods^{94,95} and expanded using Fourier techniques.⁹⁶ Neutral atom scattering factors were taken from Cromer and Waber.⁹⁷ Anomalous

dispersion effects were included in F_{calc}^{98} ; the values for $\Delta f'$ and $\Delta f''$ were those of Creagh and McAuley⁹⁹ The values for the mass attenuation coefficients are those of Creagh and Hubbell.¹⁰⁰ All calculations were performed using CrystalStructure^{101,102} except for refinement, which was performed using SHELXL-9.⁹⁴ All non-hydrogen atoms were refined anisotropically, while hydrogen atoms were introduced in calculated positions and refined on a riding model.

For **2**, one t-butyl group was disordered with two orientations (0.6 : 0.4-occupancy), and was modeled with angle restraints. Crystals of **3** were irregular and diffracted poorly leading to a high internal consistency of the reflection data. For **4**, one toluene molecule, disordered around a two-fold rotation axis, was present in the asymmetric unit. Protons could not be suitably fixed, and so they were omitted from the model, but included in the formula for the calculation of intensive properties.

For **5**, two full data collections were performed on different crystals, however, in both cases problems due to large structure size, weak diffraction (therefore, few high angle reflection/observations for refinement) and possible twinning were encountered. Due to poor internal consistency of data for the full collection, each of four scans was examined separately and only a single scan was used for solution and refinement. A second twin component, related to the first by a rotation of 2.88° around the normal to $(-2.61, -3.89, 1.00)$ was identified, however, it was not found to be significant (BASF refined to 0.0003), and was therefore not included in this model. SHELXL SIMU restraints were applied to all bonds that did not involve Al, in order to increase the observation-to-parameters ratio. The CIF file for **5** is available from the CSD where it has been deposited as a Personal Communication (F. M. Kerton, 2012, CCDC 904628).

Synthetic procedures

[ONN^{Me,tBu}]₂AlMe (1). A solution of trimethylaluminum (25% w/w in toluene; 0.270 g 3.75 mmol) was added dropwise to a rapidly stirred solution of **L1H** (2.07 g, 7.49 mmol) in toluene (10.0) mL under nitrogen at 25 °C. This mixture was allowed to stir for 2 h at room temperature, yielding a yellow solution. All volatiles were removed under vacuum affording a white solid. Yield: 1.96 g, 91.6%. X-ray quality crystals were obtained through crystallization from a 50/50 toluene/hexane solution at -35 °C. After several days, clear, colorless crystals of **1** were obtained. Anal. Calc. for C₃₅H₅₇AlN₄O₂: C, 70.91; H, 9.69; N, 9.45. Found: C, 70.65; H, 9.83; N, 9.40. ¹H NMR (C₅D₅N, 300 MHz, 298 K) δ 7.20 (2H s, ArH), 6.73 (2H, s, ArH), 3.58 (4H, s, Ar-CH₂-N), 2.35-2.59 (16H, br, N-C₂H₄-C₂H₄-N), 2.30 (6H, s, CH₃-N), 2.13 (6H, s, ArC-CH₃), 1.61 (18H, s, ArC-C{CH₃}₃), 0.12 (3H, s, Al-CH₃). ¹³C{¹H} NMR (C₇D₈, 125 MHz, 298 K) δ 155.5 (ArC-O), 138.1 (ArC-C{CH₃}₃), 136.8 (ArC-H), 126.0 (ArC-H), 123.9 (ArC-CH₂-N), 121.9 (ArC-CH₃), 62.4 (ArC-CH₂-N), 54.5 (N-C₂H₄-C₂H₄-N), 52.9 (N-C₂H₄-C₂H₄-N), 46.6 (CH₃-N), 35.4 (ArC-C{CH₃}₃), 35.3 (Al-CH₃) 31.0 (ArC-C{CH₃}₃) 30.4 (ArC-CH₃); ²⁷Al NMR (C₅D₅N, 300 MHz, 298 K) δ 74, ω_{1/2} = 4050 Hz.

[ONN^{tBu,tBu}]₂AlMe (2). This compound was prepared in the same manner as described above for **1** with trimethylaluminum (25% w/w in toluene; 0.230 g 3.14 mmol) and **L2H** (2.00 g, 6.28 mmol) as starting materials. Compound **2** was obtained as a colorless crystalline solid. Yield: 1.07 g, 77%. Crystals suitable for X-ray crystallography could be grown by cooling a saturated toluene solution at -35 °C. Anal. Calc. for C₄₁H₆₉AlN₄O₂: C, 72.74; H, 10.27; N, 8.28. Found: C, 72.75; H, 10.14; N, 8.03. ¹H NMR (C₅D₅N, 500 MHz, 328 K) δ 7.29 (2H, s, ArH), 7.08 (2H, s, ArH), 3.64 (4H, s, Ar-CH₂-N), 3.14 (8H, br, N-C₂H₄-C₂H₄-N), 2.43 (8H, br, N-C₂H₄-C₂H₄-N),

2.13 (6H, s, CH_3-N), 1.64 (18H, s, $ArC-C\{CH_3\}_3$), 1.40 (18H, s, $ArC-C\{CH_3\}_3$), -0.31 (3H, s, $Al-CH_3$); $^{13}C\{^1H\}$ NMR (C_5D_5N , 125 MHz, 298 K): δ 155.1 ($ArC-O$), 140.9 ($ArC-C\{CH_3\}_3$), 139.3 ($ArCH$), 137.4 ($ArCH$), 125.5 ($ArC-CH_2N$), 121.1 ($ArC-C\{CH_3\}_3$), 63.7 ($ArC-CH_2N$), 56.7 ($N-C_2H_4-C_2H_4-N$), 54.1 ($N-C_2H_4-C_2H_4-N$), 47.8 (CH_3-N), 36.9 ($ArC-C\{CH_3\}_3$), 36.0 ($ArC-C\{CH_3\}_3$), 33.6 ($ArC-C\{CH_3\}_3$), 32.1 ($Al-CH_3$), 31.5 ($ArC-C\{CH_3\}_3$); ^{27}Al NMR (C_5D_5N , 300 MHz, 298 K) δ 73, $\omega_{1/2} = 3490$ Hz.

[ONO^{tBu,tBu}]₂AlMe (3). Compound **3** was prepared in the same manner as described above for **2** with trimethylaluminum (25% w/w in toluene; 0.236 g, 3.27 mmol) and **L3H** (2.00 g, 6.55 mmol) as starting materials and **3** was obtained as a colorless crystalline solid. Yield: 1.92 g, 90.1%. Crystals suitable for X-ray crystallography could be grown by cooling a saturated toluene solution at -35 °C. Anal. Calc. for $C_{39}H_{63}AlN_2O_4$: C, 71.96; H, 9.76; N, 4.30. Found: C, 71.87; H, 9.77; N, 4.46. 1H NMR (C_6D_6 , 500 MHz, 343 K) δ 7.56 (2H, d, $J = 2.5$ Hz, ArH), 6.96 (2H, d, $J = 2.5$ Hz, ArH), 3.79 (4H, br, $Ar-CH_2-N$), 3.43 (8H, br, $O-C_2H_4-C_2H_4-N$), 2.91 (8H, br, $O-C_2H_4-C_2H_4-N$), 1.61 (18H, s, $ArC-C\{CH_3\}_3$), 1.40 (18H, s, $ArC-C\{CH_3\}_3$), -0.38 (3H, s, $Al-CH_3$). $^{13}C\{^1H\}$ NMR (C_6D_6 , 125 MHz, 298 K) δ 155.8 ($ArC-O$), 139.3 ($ArC-C\{CH_3\}_3$), 137.3 ($ArC-C\{CH_3\}_3$), 125.0 ($ArC-H$), 123.8 ($ArC-H$), 122.7 ($ArC-CH_2-N$), 61.3 ($ArC-CH_2-N$), 52.5 ($O-C_2H_4-C_2H_4-N$), 49.8 ($O-C_2H_4-C_2H_4-N$), 35.0 ($ArC-C\{CH_3\}_3$), 34.0, ($ArC-C\{CH_3\}_3$), 31.7 ($ArC-C\{CH_3\}_3$), 30.3 ($ArC-C\{CH_3\}_3$), 29.7 ($Al-CH_3$); ^{27}Al NMR (C_6D_6 , 300 MHz, 298 K) δ 76, $\omega_{1/2} = 4020$ Hz.

[ONN^{Me,tBu}]₂AlCl (4). Compound **4** was prepared in the same manner as described above for **2** with diethylaluminum chloride (25% w/w in toluene; 0.436 g, 3.62 mmol) and **L1H** (2.00 g, 7.23 mmol) as starting materials and **4** was obtained as a colorless crystalline solid. Yield: 1.67 g, 75.2%. Crystals suitable for X-ray crystallography could be grown by cooling a saturated toluene

solution at $-35\text{ }^{\circ}\text{C}$. Anal. Calc. for $\text{C}_{34}\text{H}_{54}\text{AlClN}_4\text{O}_2$: C, 66.59; H, 8.88; N, 9.14. Found: C, 66.32; H, 8.86; N, 8.97. ^1H NMR ($\text{C}_5\text{D}_5\text{N}$, 300 MHz, 298 K) δ 7.20 (2H s, ArH), 6.73 (2H, s, ArH), 3.59 (4H, s, Ar- CH_2 -N), 2.56 (8H, br, N- C_2H_4 - C_2H_4 -N), 2.48 (8H, br, N- C_2H_4 - C_2H_4 -N), 2.30 (6H, s, CH_3 -N), 2.25 (6H, s, ArC- CH_3), 1.59 (18H, s, ArC-C $\{\text{CH}_3\}_3$). $^{13}\text{C}\{^1\text{H}\}$ NMR (C_7D_8 , 125 MHz, 298 K) δ 155.2 (ArC-O), 136.4 (ArC-C $\{\text{CH}_3\}_3$), 128.8 (ArC-H), 128.0 (ArC-H), 127.2 (ArC- CH_2 -N), 121.8 (ArC- CH_3), 61.6 (ArC- CH_2 -N), 54.7 (N- C_2H_4 - C_2H_4 -N), 51.9 (N- C_2H_4 - C_2H_4 -N), 45.2 (CH_3 -N), 35.0 (ArC-C $\{\text{CH}_3\}_3$), 30.0 (ArC-C $\{\text{CH}_3\}_3$) 21.0 (ArC- CH_3); ^{27}Al NMR ($\text{C}_5\text{D}_5\text{N}$, 300 MHz, 298 K) δ 71, $\omega_{1/2} = 4080$ Hz.

$[\text{ONO}^{\text{tBu,tBu}}]_2\text{AlCl}$ (**5**). Compound **5** was prepared in the same manner as described above with diethylaluminum chloride (25% w/w in toluene; 0.395 g, 3.27 mmol) and **L3H** (2.00 g, 6.28 mmol) as starting materials and **5** was obtained as a colorless crystalline solid. Yield: 1.89 g, 86.3%. Anal. Calc. for $\text{C}_{38}\text{H}_{60}\text{AlClN}_2\text{O}_4$: C, 67.99; H, 9.01; N, 4.17. Found: C, 67.54; H, 9.11; N, 4.58. ^1H NMR ($\text{C}_5\text{D}_5\text{N}$, 300 MHz, 298 K) δ 7.52 (2 H, d, $J = 2.2$ Hz, ArH), 7.09 (2 H, d, $J = 2.2$ Hz, ArH), 3.67 (4H, s, ArC- CH_2 -N), 3.65 (8H, br, O- C_2H_4 - C_2H_4 -N), 2.43 (8H, br, O- C_2H_4 - C_2H_4 -N), 1.64 (18H, s, ArC-C $\{\text{CH}_3\}_3$), 1.38 (18H, s, ArC-C $\{\text{CH}_3\}_3$); $^{13}\text{C}\{^1\text{H}\}$ NMR ($\text{C}_5\text{D}_5\text{N}$, 125 MHz, 298 K) δ 154.9 (ArC-O), 141.2 (ArC-C $\{\text{CH}_3\}_3$), 139.3 (ArC-C $\{\text{CH}_3\}_3$), 124.4 (ArCH), 122.9 (ArCH), 121.1 (ArC- CH_2 -N), 66.8 (ArC- CH_2 -N), 62.5 (O- C_2H_4 - C_2H_4 -N), 53.0(O- C_2H_4 - C_2H_4 -N), 35.3 (ArC-C $\{\text{CH}_3\}_3$), 34.5, (ArC-C $\{\text{CH}_3\}_3$), 32.0 (ArC-C $\{\text{CH}_3\}_3$), 30.0 (ArC-C $\{\text{CH}_3\}_3$). ^{27}Al NMR ($\text{C}_5\text{D}_5\text{N}$, 300 MHz, 298 K) δ 73, $\omega_{1/2} = 3710$ Hz.

Typical ring-opening polymerization procedure

All manipulations were performed under an inert atmosphere. The reaction mixtures were prepared in a glove box and subsequent operations were performed using standard Schlenk techniques. A sealable Schlenk flask equipped with a stir bar was charged with a solution of complex **1** (20.0 mg, 33.7 μmol) in toluene (2.0 mL) with the prescribed amount of BnOH. Another Schlenk flask was charged with a toluene (4.0 mL) solution of ϵ -caprolactone (0.390 g, 3.37 mmol, 100 equiv). The two flasks were then attached to a Schlenk line and temperature equilibration was ensured in both Schlenk flasks by stirring the solutions for 10 minutes in a temperature controlled oil bath. The complex solution was transferred to the monomer solution, which was stirring rapidly, and polymerization times were measured from that point. At appropriate time intervals, aliquots of the reaction mixture were removed using a pipette for determining monomer conversion by ^1H NMR spectroscopy. The reaction was quenched with methanol once near-quantitative conversion had been obtained. The polymer was precipitated with an excess of cold methanol, isolated by filtration and dried under reduced pressure.

Representative copolymerization procedure

An autoclave (Parr) was heated to 80 $^{\circ}\text{C}$ under vacuum for 4 h, then cooled and moved to a glovebox. **5** (72.0 mg, 0.107 mmol) and cyclohexene oxide (5.26 g, 53.6 mmol) were placed into the autoclave, which was then sealed and removed from the glovebox. The autoclave was pressurized to 40 bar of CO_2 and was heated to the reaction temperature. After the stipulated reaction time, the reactor was cooled, vented and a small sample of the polymerization mixture was taken for ^1H NMR analysis. The remaining mixture was dissolved in dichloromethane (10 mL), quenched with methanol and then precipitated from cold methanol. The resultant polymer

was collected and dried under vacuum. Characterization of the polymer was performed by NMR and GPC. ¹H NMR (CDCl₃, 300 MHz, 298 K) δ 4.65 (br CH, polycarbonate), 3.43 (br CH, polyether), 2.2-1.1 (m CH₂, cyclohexyl).

Acknowledgements We thank NSERC of Canada, Canada Foundation for Innovation, Memorial University and the Provincial Government of Newfoundland and Labrador for financial support. S.B. thanks the Inorganic Chemistry Exchange for facilitating her research visit to Memorial University.

REFERENCES

- (1) Chandra, R.; Rustgi, R. *Prog. Polym. Sci.* **1998**, *23*, 1273.
- (2) Chen, D. R.; Bei, J. Z.; Wang, S. G. *Polym. Degrad. Stab.* **2000**, *67*, 455.
- (3) Ikada, Y.; Tsuji, H. *Macromol. Rapid Commun.* **2000**, *21*, 117.
- (4) Arbaoui A.; Redshaw, C. *Polym. Chem.* **2010**, *1*, 801.
- (5) O'Keefe, B. J.; Hillmyer, M. A.; Tolman W. B. *J. Chem. Soc. Dalton Trans.* **2001**, 2215.
- (6) Wu, J.; Yu, T.-L.; Chen, C.-T.; Lin, C.-C. *Coord. Chem. Rev.* **2006**, *250*, 602.
- (7) Labet M.; Thielemans, W.; *Chem. Soc. Rev.* **2009**, *38*, 3484.
- (8) Ajellal, N.; Carpentier, J.-F.; Guillaume, C.; Guillaume, S. M.; Helou, M.; Poirier, V.; Sarazin Y.; Trifonov, A. *Dalton Trans.*, **2010**, *39*, 8363.
- (9) Wichmann, O.; Sillanpää, R.; Lehtonen, A. *Coord. Chem. Rev.* **2012**, *256*, 371.
- (10) Ikpo, N.; Hoffmann, C.; Dawe, L. N.; Kerton, F. M. *Dalton Trans.* **2012**, *41*, 665.
- (11) Huang, Y.; Tsai, Y.-H.; Hung, W.-C.; Lin, C.-S.; Wang, W.; Huang, J.-H.; Dutta S.; Lin, C.-C. *Inorg. Chem.* **2010**, *49*, 9416.
- (12) Wang, L.; Pan, X.; Yao, L.; Tang N.; Wu, J. *Eur. J. Inorg. Chem.* **2011**, 632.
- (13) Huang C.-A.; Chen, C.-T. *Dalton Trans.* **2007**, 5561.
- (14) Kerton, F. M.; Kozak, C. M.; Luttgen, K.; Willans, C. E.; Webster R. J.; Whitwood, A. C. *Inorg. Chim. Acta.* **2006**, *359*, 2819.
- (15) Huang, C.-A.; Ho, C.-L.; Chen, C.-T. *Dalton Trans.* **2008**, 3502.
- (16) Ko B.-T.; Lin, C.-C. *J. Am. Chem. Soc.* **2001**, *123*, 7973.
- (17) Ejfler, J.; Krauzy-Dziedzic, K.; Szafert, S.; Jerzykiewicz, L. B.; Sobota, P. *Eur. J. Inorg. Chem.* **2010**, 3602.
- (18) Zhang, X.; Emge T. J.; Hultsch, K. C. *Organometallics* **2010**, *29*, 5871.
- (19) Schofield, A. D.; Barros, M. L.; Cushion, M. G.; Schwarz A. D.; Mountford, P. *Dalton Trans.* **2009**, 85.
- (20) Hung W.-C.; Lin, C.-C. *Inorg. Chem.* **2009**, *48*, 728.
- (21) Breyfogle, L. E.; Williams, C. K.; Young, J. V. G.; Hillmyer, M. A.; Tolman, W. B. *Dalton Trans.* **2006**, 928.
- (22) Marshall, E. L.; Gibson V. C.; Rzepa H. S. *J. Am. Chem. Soc.* **2005**, *127*, 6048.
- (23) Sarazin, Y.; Poirier, V.; Roisnel, T.; Carpentier, J.-F. *Eur. J. Inorg. Chem.* **2010**, 3423.

- (24) Darensbourg, D. J.; Choi, W.; Karroonnirun, O.; Bhuvanesh, N. *Macromolecules* **2008**, *41*, 3493; Liu, B.; Roisnel, T.; Guégan, J.-P.; Carpentier, J.-F.; Sarazin, Y. *Chem. Eur. J.* **2012**, *18*, 6289.
- (25) Dyer, H. E.; Huijser, S.; Schwarz, A. D.; Wang, C.; Duchateau R.; Mountford, P. *Dalton Trans.* **2008**, 32.
- (26) Amgoune, A.; Thomas C. M.; Carpentier, J.-F. *Macromol. Rapid Commun.* **2007**, *28*, 693.
- (27) Ikpo, N.; Saunders, L. N.; Walsh, J. L.; Smith, J. M. B.; Dawe, L. N.; Kerton, F. M. *Eur. J. Inorg. Chem.* **2011**, 5347.
- (28) Poirier, V.; Roisnel, T.; Carpentier, J.-F.; Sarazin, Y. *Dalton Trans.*, 2009, 9820; Poirier, V.; Roisnel, T.; Carpentier, J.-F.; Sarazin, Y. *Dalton Trans.* **2011**, *40*, 523.
- (29) Wang, L.; Ma, H. *Dalton Trans.* **2010**, *39*, 7897.
- (30) Labourdette, G.; Lee, D. J.; Patrick, B. O.; Ezhova M. B.; Mehrkhodavandi, P. *Organometallics* **2009**, *28*, 1309.
- (31) Farwell, J. D.; Hitchcock, P. B.; Lappert, M. F.; Luinstra, G. A.; Protchenko A. V.; Wei, X.-H. *J. Organomet. Chem.* **2008**, *693*, 1861.
- (32) Ejfler, J.; Szafert, S.; Mierzwicki, K.; Jerzykiewicz L. B.; Sobota, P. *Dalton Trans.* **2008**, 6556.
- (33) Doyle, D. J.; Gibson V. C.; White, A. J. P. *Dalton Trans.* **2007**, 358.
- (34) Williams, C. K.; Breyfogle, L. E.; Choi, S. K.; Nam, W.; Young, V. G.; Hillmyer, M. A.; Tolman, W. B. *J. Am. Chem. Soc.* **2003**, *125*, 11350.
- (35) Williams, C. K.; Brooks, N. R.; Hillmyer M. A.; Tolman, W. B. *Chem. Commun.* **2002**, 2132.
- (36) Chisholm, M. H.; Gallucci, J. C.; Zhen, H.; Huffman, J. C. *Inorg. Chem.* **2001**, *40*, 5051.
- (37) Chisholm M. H.; Zhou, Z. *J. Mater. Chem.* **2004**, *14*, 3081.
- (38) Lewinski, J.; Horeglad, P.; Dranka M.; Justyniak, I. *Inorg. Chem.* **2004**, *43*, 5789.
- (39) Issenhuth, J.-T.; Pluvinage, J.; Welter, R.; Bellemin-Laponnaz S.; Dagorne, S. *Eur. J. Inorg. Chem.* **2009**, 4701.
- (40) Johnstone, N. C.; Aazam, E. S.; Hitchcock, P. B.; Fulton J. R. *J. Organomet. Chem.* **2010**, *695*, 170.
- (41) Chen, H.-L.; Dutta, S.; Huang, P.-Y.; Lin, C.-C. *Organometallics* **2012**, *31*, 2016.
- (42) Bakewell, C.; Platel, R. H.; Cary, S. K.; Hubbard, S. M.; Roaf, J. M.; Levine, A. C.; White, A. J. P.; Long, N. J.; Haaf, M.; Williams, C. K. *Organometallics* **2012**, *31*, 4729.
- (43) Bouyahyi, M.; Roisnel, T.; Carpentier, J.-F. *Organometallics* **2012**, *31*, 1458.
- (44) Darensbourg, D. J.; Karroonnirun, O. *Organometallics* **2010**, *29*, 5627.
- (45) Poirier, V.; Roisnel, T.; Sinbandhit, S.; Bochmann, M.; Carpentier, J.-F.; Sarazin, Y. *Chem. Eur. J.* **2012**, *18*, 2998.
- (46) Gendler, S.; Segal, S.; Goldberg, I.; Goldschmidt, Z.; Kol, M. *Inorg. Chem.* **2006**, *45*, 4783.
- (47) Groysman, S.; Sergeeva, E.; Goldberg I.; Kol, M. *Inorg. Chem.* **2005**, *44*, 8188.
- (48) Broomfield, L. M.; Sarazin, Y.; Wright, J. A.; Hughes, D. L.; Clegg, W.; Harrington, R. W.; Bochmann, M. *J. Organomet. Chem.* **2007**, *692*, 4603.
- (49) Platel, R. H.; Hodgson, L. M.; Williams, C. K. *Polym. Rev.* **2008**, *48*, 11.
- (50) Yu, R.-C.; Hung, C.-H.; Huang, J.-H.; Lee, H.-Y.; Chen, J.-T. *Inorg. Chem.* **2002**, *41*, 6450.
- (51) Ma, W.-A.; Wang, Z.-X. *Organometallics* **2011**, *30*, 4364.

- (52) Collins, K. L.; Corbett, L. J.; Butt, S. M.; Madhurambal, G.; Kerton, F. M. *Green Chem. Lett. Rev.* **2007**, *1*, 31.
- (53) Kerton, F. M.; Power, A.; Soper, R. G.; Sheridan, K.; Lynam, J. M.; Whitwood A. C.; Willans, C. E. *Can. J. Chem.* **2008**, *86*, 435.
- (54) Delpuech, J. J.; in *NMR of Newly Accessible Nuclei* Laszlo, P. Ed. Academic Press: New York, **1983**, Vol 2, Chapter 6.
- (55) The connectivity of complex **5** is supported by an X-ray diffraction study but the quality of this prevents its publication; Private Communication, F. M. Kerton, 2012, CCDC 904628.
- (56) Addison, A. W.; Rao, T. N.; Reedijk, J.; van Rijn, J.; Verschoor, G. C. *J. Chem. Soc., Dalton Trans.* **1984**, 1349.
- (57) Gao, A.; Mu, Y.; Zhang, J.; Yao, W. *Eur J. Inorg. Chem.* **2009**, 3613.
- (58) Hogerheide, M. P.; Wesseling, M.; Jastrzebski, J. T. B. H.; Boersma, J.; Kooijman, H.; Spek, A. L.; van Koten, G. *Organometallics* **1995**, *14*, 4483.
- (59) Kumar, R.; Sierra, M. L.; Oliver, J. P. *Organometallics* **1994**, *13*, 4285.
- (60) Chen, C.-T.; Huang, C.-A.; Huang, B.-H. *Dalton Trans.* **2003**, 3799.
- (61) Sun, W.-H.; Shen, M.; Zhang, W.; Huang, W.; Liu, S.; Redshaw, C. *Dalton Trans.* **2011**, *40*, 2645.
- (62) Mata-Mata, J. L.; Gutiérrez, J. A.; Paz-Sandoval, M. A.; Madrigal A. R.; Martínez-Richa, A. *J. Polym. Sci. Part A: Polym. Chem.* **2006**, *44*, 6926.
- (63) Tai, Y.-E.; Li, C.-Y.; Lin, C.-H.; Liu, Y.-C.; Ko, B.-T.; Sun, Y.-S. *J. Polym. Sci. Part A: Polym. Chem.* **2011**, *49*, 4027.
- (64) Martin, E.; Dubois, P.; Jerome, R. *Macromolecules* **2000**, *33*, 1530.
- (65) Normand, M.; Kirillov, E.; Roisnel, T.; Carpentier, J.-F. *Organometallics* **2012**, *31*, 1448 and references therein.
- (66) Duda, A. *Macromolecules* **1994**, *27*, 576.
- (67) Duda, A. *Macromolecules* **1996**, *29*, 1399.
- (68) Zhang, C.; Wang, Z.-X. *J. Organomet. Chem.* **2008**, *693*, 3151.
- (69) Zhang, C.; Wang, Z.-X. *Appl. Organometal. Chem.* **2009**, *23*, 9.
- (70) Albertsson, A.-C.; Varma, I. K. *Biomacromolecules* **2003**, *4*, 1466.
- (71) Takeuchi, D.; Nakamura, T.; Aida, T. *Macromolecules* **2000**, *33*, 725.
- (72) Dubois, P.; Jacobs, C.; Jerome, R.; Teyssie, P. *Macromolecules* **1991**, *24*, 2266.
- (73) Darensbourg, D. J.; Ganguly, P.; Billodeaux, D. *Macromolecules* **2005** *38*, 5406.
- (74) Kerton, F. M.; Whitwood, A. C.; Willans, C. E. *Dalton Trans.*, **2004**, 2237.
- (75) Yao, W.; Mu, Y.; Gao, A.; Su, Q.; Liu Y.; Zhang, Y. *Polymer* **2008**, *49*, 2486.
- (76) Luftmann, H.; Rabani, G.; Kraft, A. *Macromolecules* **2003**, *36*, 6316-6324.
- (77) Piskun, Y. A.; Vasilenko, I. V.; Kostjuk, S. V.; Zaitsev, K. V.; Zaitseva G. S.; Karlov, S. S. *J. Polym. Sci. Part A: Polym. Chem.* **2010**, *48*, 1230.
- (78) Yang, X.; Wang, L.; Yao, L.; Zhang, J.; Tang, N.; Wang, C.; Wu, J. *Inorg. Chem. Commun.* **2011**, *14*, 1711.
- (79) Liao, T.-C.; Huang, Y.-L.; Huang, B.-H.; Lin, C.-C. *Macromol. Chem. Phys.* **2003**, *204*, 885.
- (80) Chen, H.-L.; Ko, B.-T.; Huang, B.-H.; Lin, C.-C. *Organometallics* **2001**, *20*, 5076.
- (81) Dakshinamoorthy, D.; Peruch, F. *J. Polym. Sci., Part A: Polym. Chem.* **2011**, *49*, 5176.
- (82) Zhong, Z.; Dijkstra, P. J.; Birg, C.; Westerhausen, M. Feijen, J. *Macromolecules* **2001**, *34*, 3863.

- (83) Duda, A.; Penczek, S. *Macromolecules* **1995**, *28*, 5981.
- (84) Chmura, A. J.; Davidson, M. G.; Jones, M. D.; Lunn, M. D.; Mahon, M. F.; Johnson, A. F.; Khunkamchoo, P.; Roberts, S. L.; Wong, S. S. F. *Macromolecules* **2006**, *39*, 7250.
- (85) Li, W.; Wu, W.; Wang, Y.; Yao, Y.; Zhanga, Y.; Shen, Q. *Dalton Trans.* **2011**, *40*, 11378.
- (86) Gong, S.; Ma, H. *Dalton Trans.* **2008**, 3345.
- (87) Duda, A.; Florjanczyk, Z.; Hofman, A.; Slomkowski, S.; Penczek, S. *Macromolecules* **1990**, *23*, 1640.
- (88) Dubois, P.; Ropson, N.; Jerome, R.; Teyssie, P. *Macromolecules* **1996**, *29*, 1965.
- (89) Iwasa, N.; Katao, S.; Liu, J.; Fujiki, M.; Furukawa, Y.; Nomura, K. *Organometallics* **2009**, *28*, 2179.
- (90) Darensbourg, D. J.; Karroonnirun, O.; Wilson, S. J. *Inorg. Chem.* **2011**, *50*, 6775.
- (91) Dagonne, S.; Bouyahyi, M.; Vergnaud, J.; Carpentier, J.-F. *Organometallics* **2010**, *29*, 1865.
- (92) Selected reviews: Darensbourg, D. J. *Chem. Rev.* **2007**, *107*, 2388; Kember, M. R.; Buchard, A.; Williams, C. K. *Chem. Commun.* **2011**, *47*, 141; Lu, X.-B.; Darensbourg, D. J. *Chem. Soc. Rev.* **2012**, *41*, 1462
- (93) Selected papers on CO₂ copolymerization using Al complexes: Darensbourg, D. J.; Billodeaux, D. R. *Inorg. Chem.* **2005**, *44*, 1433; Aida, T.; Inoue, S. *Acc. Chem. Res.* **1996**, *29*, 39; Aida, T.; Ishikawa, M.; Inoue, S. *Macromolecules* **1986**, *19*, 8
- (94) SHELX97: Sheldrick, G.M. *Acta Cryst.* **2008**, *A64*, 112.
- (95) SIR92: Altomare, A.; Casciarano, G.; Giacovazzo, C.; Guagliardi, A.; Burla, M.; Polidori, G.; Camalli, M. *J. Appl. Cryst.* **1994**, *27*, 435.
- (96) DIRDIF99: Beurskens, P.T.; Admiraal, G.; Beurskens, G.; Bosman, W. P.; de Gelder, R.; Israel R.; Smits, J. M. M. *The DIRDIF-99 program system, Technical Report of the Crystallography Laboratory, University of Nijmegen, The Netherlands, 1999.*
- (97) Cromer D. T.; Waber, J. T. *"International Tables for X-ray Crystallography", Vol. IV, The Kynoch Press, Birmingham, England, 1974, Table 2.2 A.*
- (98) Ibers J. A.; Hamilton, W.C. *Acta Cryst.* **1964**, *17*, 781.
- (99) Creagh, D. C.; McAuley, E. W. J. *"International Tables for Crystallography", Vol C, (A.J.C. Wilson, ed.), Kluwer Academic Publishers, Boston, 1992, Table 4.2.6.8, page 219.*
- (100) Creagh, D. C. Hubbell, J. H. *"International Tables for Crystallography", Vol C, (A.J.C. Wilson, ed.), Kluwer Academic Publishers, Boston, 1992, Table 4.2.4.3, page 200.*
- (101) CrystalStructure 3.7.0: Crystal Structure Analysis Package, Rigaku and Rigaku/MSU (**2000-2005**). 9009 New Trails Dr. The Woodlands TX 77381 USA.
- (102) Watkin, D. J.; Prout, C. K.; Carruthers, J. R.; Betteridge, P. W. *CRYSTALS Issue 10: Chemical Crystallography Laboratory, Oxford, UK. 1996.*